The significance of fluoride uptake and inflammation within the atherosclerotic plaque: a PET/CT analysis

Dottorato di Ricerca in Medicina Interna
XXXI Ciclo
Curriculum: Fisiopatologia delle Malattie Cardiovascolari e Renali

Tesi Finale

Candidato
Dott. Francesco Fiz

Relatore
Ch.mo Prof. Marcello Bagnasco

Università degli Studi di Genova
Dipartimento di Medicina Interna (DIMI)

"Die Logik ist zwar unerschütterlich, aber einem Menschen, der leben will, widersteht sie nicht."

F.Kafka, Der Prozess

Abstract

Background and aims: Atherosclerosis is a vessel disease, having a relatively early onset and a slow progression, and is currently the first cause for morbidity and mortality worldwide. Patients with atherosclerosis are usually classified according to their cardiovascular risk; however, tools to characterize the atherosclerotic plaque or to predict its progression are presently missing. In this thesis, we present a novel approach to this issue, by applying multimodal (CT- ad PET-based) imaging, in synergy with segmentation analysis, to the atherosclerotic plaques.

Materials and Methods: Patients were recruited from three different databases retrospectively and then assigned to three different study populations. Population A consisted of 51 patients (19 females, mean age 69±9 years, range 49-82), submitted to ^{18}F-NaF-PET/CT (NaF-PET). Each patient underwent at least 2 Naf-PET, spaced on average 14 months apart. In each patient, a VOI was placed on each visible CT plaque, using a CT-iso-contour approach; mean blood-pool normalized SUV (TBR), mean HU and Agaston-like calcification score (CS) were computed. TBR was compared with the mean percent variation of HU and CS, normalized for elapsed time between NaF-PETs (NDHU% and NDCS%, respectively). Whole-aorta TBR was then compared to whole-aorta NDCS%.

Population B included 79 patients (51 women, 70.8 ±8 years) who underwent NaF-PET. Plaque analysis was performed as described above. An in-house software application was used to identify and segment the trabecular bone semi-automatically. TBR and HU of trabecular bone were compared to the ones of arterial plaques.

Population C consisted of twenty-seven patients (12 males, mean age 69.4 ± 8, range 56-87), who underwent a 18F-FDG and a 68Ga-DOTATOC PET/CT within a two-weeks period.

Cardiovascular risk score was estimated in all patients; TBRmax and TBRmean was calculated in a large VOI, placed on the aorta, in FDG and DOTATOC scans.

Results: In population A, mean HU and CS significantly increased from the first to the second PET/CT ($p<0.001$). A tight and direct correlation was noted between TBR in the plaques in the baseline PET and both NDHU% ($R=0.67$, $p<0.01$) and NDCS% ($R=0,7$, $p<0.001$). Whole-aorta TBR correlated with NDCS% in the entire vessel ($R=0,85$, $p<0.001$).

In the population B, mean plaque density showed an inverse association with vertebral HU density ($R=-0.56$, $p<0.01$). Plaque and trabecular bone TBR were directly and closely correlated ($R=0.63$ and $p<0.001$). At univariate analysis, mean HU density of aortic plaque was not predicted by any of the cardiovascular risk factor or by age; conversely, it was related to its own TBR ($p=<0.001$) as well as by trabecular bone TBR.

In population C, the mean of TBRmax was significantly higher in 68Ga-DOTATOC PET, when compared to FDG ($5,7\pm3,1$ Vs. $2\pm1,2$, $p<0.01$). A tight and direct correlation was noted between FDG TBRmean and CV risk score ($R=0.82$, $p<0.001$), as well as between 68Ga-DOTATOC TBRmean and CV risk score ($R=0.81$, $p<0.001$). Average TBRmax of 68Ga-DOTATOC was slightly higher in DM patients when compared to the non-diabetic ones (6 ± 2.1 Vs. $4,9\pm0,9$, $p<0.05$).

Conclusions: PET/CT with NaF can predict subsequent plaque evolution: in particular, plaque displaying a higher uptake have a greater progression of calcification at follow-up. Observing the behavior of skeletal bone might represent a new window for assessing the plaques´ characteristics. Inflammation within the plaque can be detected by ^{18}F-FDG and by ^{68}Ga-DOTATOC, the latter tracer might perform better, especially in diabetic patients. Overall PET techniques could display a great relevance in diverse research fields, such as assessment of therapy effectiveness and identification of vulnerable plaques; further study could allow the application of this methods to larger population,

possibly enabling a patient-centered treatment and improving therapy outcomes as well as quality of life.

Table of Contents

INTRODUCTION

Cardiovascular disease: the size of the phenomenon

One of the most abused *incipits* of each cardiovascular research item is the constant reference to the sky-rocketing prevalence of cardiovascular (CV) disease. However, this statement is to this day true, even though its prevalence in western countries is somewhat reaching a *plateau* [1]. When morbidity and mortality of cardiovascular and cerebrovascular diseases are considered as one entity, their social and economic burden exceeds by far the one caused by all neoplastic diseases combined [2; 3]. To size the phenomenon up, one must consider that CV disease, as reported by the Global Burden of Disease Study 2015, accounts for about 23 millions of deaths and roughly 500 millions of disability-adjusted life years globally. Among these events, two third are caused by cardiovascular, and one third is caused by cerebrovascular accidents. A complete overview of the statistics, adjustable for the various parameter of the global population, can be found online, using a practical search tool: https://gbd2016.healthdata.org/gbd-search/.

Moreover, the incidence and prevalence of CV disease might further increase in the years to come, when appropriate measures are not implemented [4]. Even though many health-related indicators are bound to improve in the near future, some of them, such as BMI, are currently progressively worsening and might contribute to aggravating the disease burden in the aging population.

It is evident that such a condition represents one of the most significant challenges of the present-day medicine: reducing the impact of CV disease could contribute to limit the huge cost due to the required healthcare and the years of disability [5]. Moreover and more importantly, the magnitude of the problem is not currently matched by an appropriate volume, quality and methodology of clinical research, as a large part of the available

evidence derives from small-scale retrospective studies, with insufficient statistical power to guide a translational approach to the CVD pathology [6].

The cardiovascular patient: a black box of risk factors

Since the dawn of modern internal medicine, the prevention of CVD progress has been focused on treating cardiovascular (CV) risk factors [7]. These factors classically include increased body mass index, hypertension, elevated cholesterol levels, impaired glucose tolerance or diabetes, and smoking habit; family history for CVD also plays a role [8]. Together, presence and degree of these indices concur to profile the risk for an acute cardiovascular event that a given patient faces [9]. This score represents the likelihood of an acute event, based on the patient's clinical characteristics: it does not tell the physician whether an underlying cardiovascular disease is present or whether a known CV condition is progressing. A patient with a high CVR might live to the end of her or his days without any cardiological problem or might die from another cause; conversely, a patient with low risk might face an acute event, which could affect his or her future quality of life. To complicate the matter, some acute events could occur without symptoms, especially in diabetic patients [10] [11]. The task of the clinician is to treat the existing risk factors at the best of his or her possibilities; however, the uncertainty about the patients' compliance and the relative difficulty to evaluate the underlying pathology complicate the prevention of CV events. This last point must be described in detail.

The arterial plaque: a life-long history

Cardiovascular disease is characterized by the progressive narrowing of blood vessels, which, at first, might produce symptoms only during the phases of maximal flow, such as exercise;

later on, the stenosis might get so advanced to restrict blood flow even at rest [12]. This phenomenon is caused by the insurgency and the progression of the atherosclerotic plaque, which develops in the inner vessel *intima* and slowly grows towards the center of the vessels, causing the above-mentioned progressive obstruction [13]. The process of atherosclerotic formation is not a rapid one. Although cardiovascular and cerebrovascular diseases are ailments of the elderly, there is a large body of evidence indicating that the activity of plaque build-up begins at an early age. In particular, studies that were carried out on members of the US armed forces that have perished in combat at an early age (mean 25.9 years) revealed a relevant prevalence (8.5%) of coronary atherosclerosis; 2.3% of all soldiers presented an advanced coronary artery disease [14]. Evidence of beginning atheromatosis has been found in the pediatric population as well [15]. These data depict an upsetting picture: if the cardiovascular disease is so widespread, how can the physician recognize the progressing CVD and adopt adequate countermeasures?

The diagnostic arsenal: from electrophysiology to invasive diagnostic

Having defined a patient as a CV risk-bearer, which steps are to be taken in order to properly diagnose a significant CVD? Patients presenting at least an intermediate risk for cardiovascular disease should receive further testing. In particular, those with intermediate risk benefit from non-invasive testing, such as stress EKG [16]. This test is performed by having the patient exercise, using a treadmill or an bicycle ergometer, or by inducing vasodilation with a pharmacologic agent: these measures cause an increase in the blood flow in normal vessels. Conversely, in vessels affected by atherosclerosis, the flow is reduced (as the vasodilation in healthy vessels induces the so-called “coronary steal syndrome”). The reduced perfusion produces ischemic damage in the affected area: this alteration perturbates the electrical conduction of the heart contraction impulse; which is picked up by

the EKG device and might be revealed as an alteration of the ST-segment. Stress testing is reasonably safe and can be coupled to imaging, such as echocardiography or radioisotope perfusion imaging; however, the present a suboptimal sensitivity of 70% and a low specificity of 50-70% [17]. This means that a relevant proportion of patient with CAD will not be correctly diagnosed and that an even greater proportion will be sent to invasive imaging for no reason. These figures can be improved by coupling the stress test with radioisotope perfusion imaging [18], where a radioactive tracer is injected at the exercise peak and under rest condition: comparison of the two image sets allows identifying areas of reduced myocardial perfusion under an increased workload. Nuclear imaging offers a multiparameter examination, being able to estimate heart perfusion and contractility within a single examination; however, it is not able to provide information about the presence and characteristics of the underlying plaque pathology.

Patient with a high risk for CVD or patients that test positive at first-line screening must undergo an invasive procedure, e.g., coronarography. This examination is performed by guiding an arterial catheter to the origin of the coronary arteries; here, a bolus of contrast medium is repeatedly injected under x-ray imaging, granting a vision of the coronary tree and an estimation of the blood flow. The advantages of this procedure include high sensitivity and the possibility to perform a therapeutic procedure (such as balloon dilation or stenting); the disadvantage include a non-neglectable risk for complication and the impossibility to visualize, under basal conditions, the arterial plaque directly [19; 20].

Other non-invasive methods are based on detection of plaque and luminal stenosis using x-ray computed tomography (CT). Basically, non-enhanced CT can be used to detect calcium deposition within the coronary arteries, as these deposits are associated with plaques and present a high, bone-like attenuation coefficient [21]. Coronary calcium score (CS), which is

obtained through an algorithm, applied on CT images, can predict the risk of major adverse cardiovascular events (MACE) [22]. However, it is unable to tell whether an individual plaque is about to rupture, and it grants no information on the degree of stenosis, perfusion, and coronary flow reserve. Such information may be obtained from CT-angiography, which is superior to CS determination in forecasting the MACE likelihood [23]. Nevertheless, its greatest value lays in its high negative predictive value; positive scans have however to be confirmed by invasive coronarography [24].

Overall all these electrophysiological, radiological and radioisotope methods are very effective in describing the effects of atherosclerosis on the cardiovascular system but offer little or no information on the primary cause of the CVD, i.e. the atherosclerotic plaque.

The plaque microcosm: a matter of paramount importance in predicting MACE

The matter of plaque composition is in no way a trivial one [25]. In fact, despite the large prevalence of atherosclerosis, only a percentage of individual will face an acute event [26]. It has been demonstrated that is not the present or the extent, but rather the composition of a plaque which determines the risk for MACE [27]. The plaque represents a tiny universe of complex interactions between different cells types, risk factors, and genetic predisposition: this complexity account for the difficulty to establish the risk purely through mere morphological imaging [28]. The pathophysiology of the arterial plaque development has been already widely and thoroughly described, with the first reports being over 150 years old [29]. Briefly, the process is usually started by LDL migrating into the sub-endothelium; here an oxidation process is started, which in turn releases cytokines and growth factors that attract monocytes [30]. “Foam” cells start accumulating and smooth muscle cells proliferate, constituting the core of the growing plaque [31]. In parallel, the chronic inflammation

triggers a differentiation path in mesenchymal progenitors, which become committed to the osteoblast line; the same mechanisms produce an osteoclast differentiation from hematopoietic stem cells [32]. These mechanisms ultimately produce the plaque calcification, which is then apparent at CT imaging and that is associated with end-stage plaque evolution. In fact, these mechanisms are prevalent in the earlier phases of plaque evolution. When the calcifications progress, then the plaque becomes hypocellular and the calcium deposition might further progress only with "passive" mechanism, as the endothelium gets no longer able to impede calcium salt precipitation [33]. Under certain conditions, the plaque might rupture, its core might become exposed and trigger a cascade of coagulation phenomena [34].

Classifying the plaques' behavior: the role of hybrid imaging

Since the plaque represents an active, ever-changing microenvironment, it follows that employing morphological imaging techniques might, at best, succeed in obtaining a snapshot of a certain moment in the plaque history. However, no data on the plaque tendency to growth, or on the likelihood to cause an acute event will be obtained.

In recent years, the question has been however tackled by hybrid (morphological and radioisotope) imaging. The progress made with PET/CT devices has allowed combining the anatomic information with the functional one, with an unprecedented spatial resolution. Many aspects of the plaque have been investigated up to this day. The first studies dealt with the identification of plaque inflammation, using ^{18}F-fluorodeoxyglucose (FDG) as a tracer [35; 36]. However, FDG presents some limitations, the most important of which is the intensive uptake within the myocardium, which reduces the possibility to obtain accurate readings from plaques adjacent to the myocardial wall [37]. Other limitations include statin

treatment and diabetes mellitus. Therefore, the possibility to investigate inflammation with somatostatin-receptor tracers was explored. In fact, activated macrophages express these receptors on their surface: this feature should be much more specific than mere glucose consumption as measured by FDG-PET [38]. Using 68Ga-DOTATATE, Tarkin and colleagues managed to identify “culprit” arteries after acute myocardial or cerebrovascular events; moreover, tracer uptake correlated with the cardiovascular risk score. However, another paper, which conducted an analysis of 68Ga-DOTATATE uptake within plaques two days after an acute carotid event, found no difference between culprit and non-culprit plaques [39]. The discrepancy might be caused by the different sample size or by the different phase of activation of the macrophages within the plaque.

Inflammation represents, in fact, an intermittent phenomenon. Conversely, whereas calcification shows a later onset, it might indeed show a steadier progression that may allow the identification of the increased metabolism associated with plaque reparation after an acute event. For this reason, a great number of studies dealing with plaque uptake of ^{18}F-Natrium fluoride (NaF) have been conducted in the last decade [33; 40-45]. These studies demonstrated the feasibility of the method and the correlation of fluoride uptake with cardiovascular risk factors; moreover, they also demonstrated that such PET imaging shows the greatest effectiveness in plaques displaying light to moderate calcification (as the old, clumped calcium deposits have not enough cellularity to exhibit an adequate tracer uptake). Finally, a brilliant study from Joshi and co-worker demonstrated that NaF localizes into the culprit plaque after a MACE; the bone-seeking agent also shows a correlation with bone-forming factors within the plaque [46].

In general, analyses conducted with PET tracers tried to clarify first whether tracking plaque metabolism was feasible and then whether plaque with suspect features could be identified.

The first point has been doubtlessly a success: signal from the atherosclerotic lesion can be identified and quantified with a number of tracers, thanks to the improved acquisition and reconstruction protocols for PET imaging. However, the significance of this information has not yet been established. This point is fundamental for translational purposes, i.e. moving the plaque analysis to bedside. In order to do so, one has to identify a possible impact of plaque uptake on the disease's progress.

In this doctoral thesis, a longitudinal analysis of PET uptake within plaque will be carried out, so as to identify whether plaque uptake reflects the future plaque evolution. To this purpose, serial PET will be analyzed, to measure the modifications in plaque density and tracer uptake over time. Furthermore, regions of increased uptake without visible calcium deposition, which may represent non-yet-calcified plaques, will also be studied.

The field of research will then be expanded to the entire body: as atherosclerosis is a systemic disease, the correlation between calcium content and uptake within plaque and trabecular bone will be studied. In fact, a correlation between arterial calcium deposition and atherosclerosis has been shown. When a metabolic link between the two systems should be confirmed, then targeted bone-active therapies could be tested, to try and prevent plaque evolution.

Finally, FDG and somatostatin receptors will be pitted against each other, to gain knowledge of which one is the aptest for plaque inflammation imaging.

STUDY OBJECTIVES

Aim 1: To verify whether fluoride uptake in atherosclerotic plaques corresponds to a subsequent variation of their calcium content at follow-up studies. To assess whether regions of increased tracer uptake within the vessel wall show a higher density score when compared to segments without uptake. To ascertain whether focal NaF uptake might signal the future insurgence of an arterial plaque.

Aim 2: To test the correlation between plaque and trabecular bone. To do so, plaque characteristics will be studied. Bone features will be assessed by employing an in-house coded software application, able to identify the trabecular bone in the CT images automatically, and to extract the metabolic information from the co-registered PET images.

Aim 3: To study the correlation between glucose intake and expression of somatostatin receptors, as a measure of active inflammation, within the arterial plaque. Data will be stratified by vessels region and patients' risk factors.

MATERIALS AND METHODS

In order to carry out the objectives stated in the "Aims", patients were recruited retrospectively from three different databases and distributed into three different study group, each named with a letter (A, B and C for the Aims 1, 2 and 3, respectively). The analysis was carried out offline and on anonymized data. In all patients, written informed consent was obtained from each patient before the exam, including the permission to use pseudonomyzed imaging data for research purpose. Institutional Ethics Committee approved the analysis in all cases and the requirement to obtain additional informed consent for this specific analysis was waived.

The populations consisted generally of oncologic patients, affected by confirmed metastatic prostate or breast cancer (populations A and B) or by metastatic NET (population C). The databases were located and contained data of patients whose examination had been carried out at the following nuclear medicine units:

- Department of Health Sciences (DISSAL), University Hospital "IRCCS-San Martino-IST", Genoa, Italy
- "Duchessa di Galliera" General Hospital, Genoa, Italy
- "Sant Andrea" General Hospital, La Spezia, Italy

Population A

General Characteristics

The population consisted of 51 patients (19 females, mean age 69±9 years, range 49-82), affected by metastatic prostate or breast cancer. Each patient underwent at least two consecutive NaF PET/CT examinations; 15 patients (29%) had at least three exams and 7 patients (14%) had four or more PET/CT. On average PET/CT examinations were spaced 14

months apart (range 6-40). Exclusion criteria were: history of vasculitis, autoimmune or systemic inflammatory disease as well as chemo- or radiotherapy in the 8 weeks preceding each PET/CT examination. Patients having baseline and follow-up studies performed with different CT protocols or whose PET images were reconstructed with different methods were excluded from the analysis.

Image acquisition and reconstruction

Patients underwent 18F-NaF PET/CT using two 16 slices PET/CT hybrid systems: (1) Biograph 16 (Siemens Medical Solutions, Knoxville TN, United States); and (2) Discovery LS (GE Medical Systems, Milwaukee, WI, United States). In both cases patients received an intravenous bolus injection of 18F-NaF (4.8-5.2 MBq per kilogram of body weight). PET/CT acquisition started 60-75 min thereafter, in the meantime the patient was hydrated and encouraged to void, as to diminish the unbound tracer fraction. The entire body was scanned from vertex to toes in an “arms down” position; emission scan lasted 120’’ per bed position. PET raw data were reconstructed by means of ordered subset expectation maximization (OSEM, 3 iterations, 16 subsets) and attenuation correction was performed using CT data. The transaxial field of view and pixel size of the reconstructed PET images were 58.5 cm and 4.57 mm, respectively, with a matrix size of 128 × 128 mm. As per standard PET/CT imaging protocol, 16-detector row helical CT scan was performed with non-diagnostic current and voltage settings (120 Kv, 80 mA), with a gantry rotation speed of 0.5 s and table speed of 24 mm per gantry rotation. No contrast medium was injected. The entire CT dataset was fused with the 3-dimensional PET images using an integrated software interface (Syngo; Siemens Erlangen, Germany). Low dose CT (reconstructed at 4mm thick slices) was used for anatomical reference for the localization of vascular calcification.

Image Analysis

Images were analyzed at a research workstation using the Horos DICOM viewer (Pixmeo Sàrl, Bernex, CH). On each patient, fusion (PET and CT) and CT images of the baseline and of the follow up study were opened in parallel. The slice position was synchronized at the appearance of the vertex. The images were then scrolled, to identify presence of calcification within the abdominal aorta wall. All isolated calcifications (AC) were identified, calcifications with evidence of tracer spillover from the vertebrae were excluded (a minimum distance of 1 cm from any vertebral body was in all cases required). Also, immense, clumped and ring-like calcifications, stretching for more than 5 CT consecutive slices, were excluded due to their low likelihood of presenting cellularity capable of tracer uptake [33]. On each AC, a VOI was built semi-automatically, using a 3D region-growing algorithm (Figure 1).

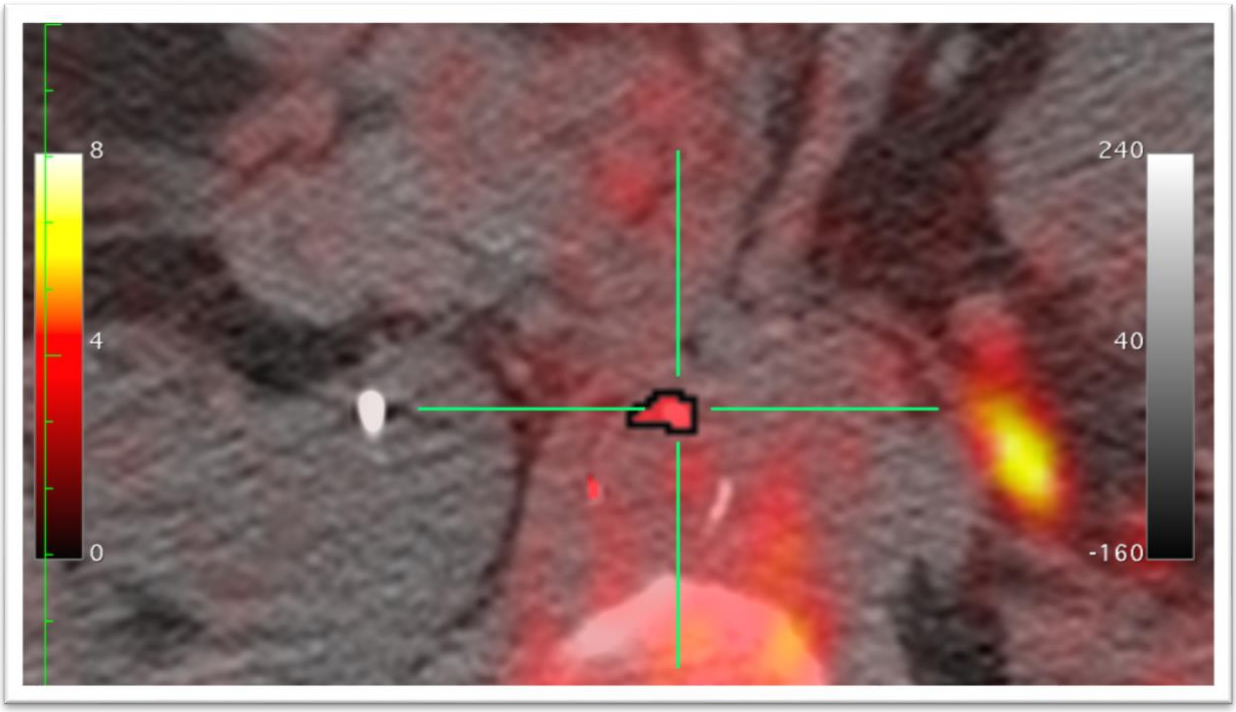

Figure 1. VOI creation on arterial plaques. Volumes were created using a region-growing algorithm: once set a seeding point, the software toll will generate a VOI by including all neighboring voxels above a certain HU threshold.

In each VOI, mean SUV and mean HU density were computed. Additionally, an Agaton-like CS was calculated, using a dedicated Horos plug-in. Mean SUV was normalized for blood pool (BP), to account for different uptake time, for different scanners and to adjust for detectors' sensitivity. Blood pool was obtained by manually drawing a 10-slice thick VOI in the inferior vena cava, the SUV/BP ratio was defined target-to-background ratio (TBR).

The same plaque was then identified on the follow-up scan and a similar VOI was constructed. Percent difference in HU and CS was calculated and named Delta-HU (DHU%) and Delta-CS (DCS%). These two values were in turn normalized for the number of months elapsed between scans (NDHU% and NDCS%, respectively).

Finally, a large VOI, comprising the entire abdominal aorta, was drawn (while maintaining the ground rule of keeping a 1 cm distance from the vertebrae) and the BP normalized SUV was calculated (TBR). Within the same space, the total CS was calculated, by applying the tool to each calcium deposition within the vessel wall and by summing the results.

Statistical Analysis

All data are reported as Mean ± SD. Differences between groups were tested using one-way analysis of variance, with intergroup comparison afforded using Bonferroni test. Paired T-Test was used to assess the variation of uptake, HU, and CS in the plaques (test-retest). Correlation was tested used bivariate analysis (Pearson's R as well as by multiple linear regression analysis). p values <0.05 were considered as statistically significant. Statistical analyses were performed using SPSS software Advanced Models 24 (IBM, Chicago, Illinois, US).

Population B

General Characteristics

The study included 79 patients with either breast (65%) or prostate (35%) cancer undergoing 18F-NaF PET/CT scan for suspected bone metastases or for monitoring of known ones. Patients were included in the analysis if they presented at least one CT-evident arterial calcification (AC) in the infrarenal abdominal aorta. AC was defined as described above (see Population A).

Exclusion criteria were: history of vasculitis, autoimmune or systemic inflammatory disease as well as chemo- or radiotherapy in the preceding 8 weeks, as previously proposed. Chronic steroid therapy represented an additional exclusion factor. Cardiovascular risk profile was assessed in each patient (including age, sex, diabetes, smoking, hypertension, dyslipidemia and body mass index).

35 age- and sex-matched patients, having no evidence of arterial calcifications were randomly selected from our pool of 18F-NaF-PET/CT examinations and used as plaque-free controls.

Image Analysis

Plaque analysis was carried out as described above.

Bone image analysis was performed semi-automatically according to a previously validated method [47]. Briefly, the algorithm identifies the skeleton on CT images assuming that compact bone is the structure with the highest radiograph attenuation coefficient in the human body. Once it has identified the skeletal border, the program starts the thresholding algorithm, which samples a 2-voxel- thick layer and computes its average Hounsfield Unit (HU) value. Thereafter, all skeletal voxels having attenuation coefficient equal or above this value are considered as compact bone, and the remaining as trabecular bone. This latter

volume is then voxel-wise multiplied against the PET co-registered data to extract and represent bone marrow metabolic activity. For the purpose of the present analysis, thoracic and lumbar vertebrae were selected as representative bone regions.

This above-described segmentation method can tell apart osteoblastic metastases from normal trabecular bone [33]. Moreover, the software removes all voxels under a 100 HU threshold, effectively excluding lytic metastases. Therefore, it is possible to analyze trabecular bone metabolism without the influence of uptake from tumor localizations. However, effects due to radioactivity spill-over from nearby lesion or presence of mixed-type metastases within trabecular bone cannot be denied with utmost security by the automated analysis. For this reason, two expert readers reviewed the output images and manually removed all bone regions with suspicious metastatic involvement.

See Figure 2 for a graphical representation of the bone marrow analysis.

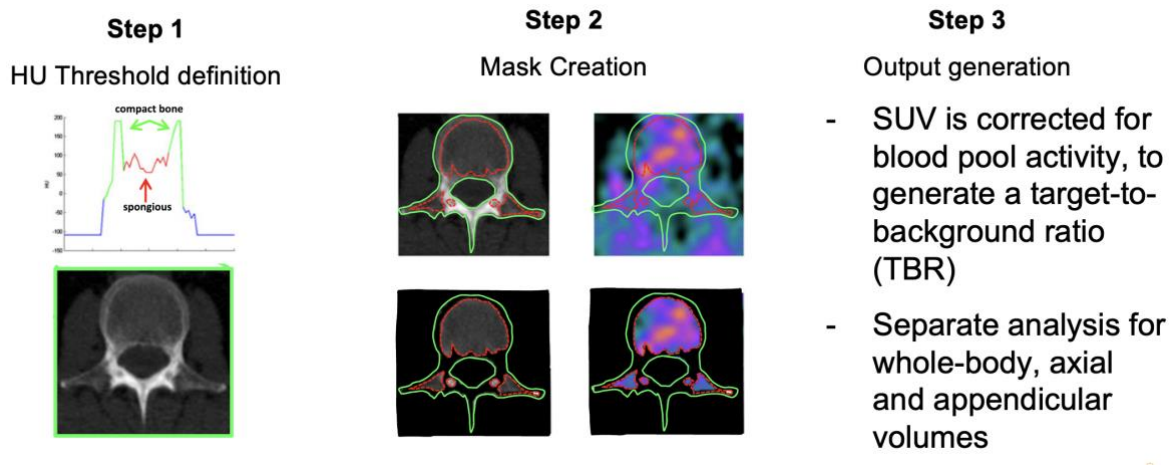

Figure 2. Analysis of the trabecular bone activity. A MatLab-based computational tool was applied to the PET/CT images. The application identifies and segments the trabecular space automatically. It then generates a mask, which is copied onto the PET dataset, allowing the extraction of functional information exclusively from the target bone tissue.

Statistical Analysis

All data are reported as Mean ± SD. Patients with ACs were stratified in three groups according to their tercile of mean plaque density: patient with a mean calcification in the

lower tercile were defined as with “light” calcifications, while those in the middle and upper terciles were defined as having “medium” and “heavy” calcifications, respectively.

Differences between groups were tested using one-way analysis of variance, with intergroup comparison afforded using Bonferroni test. Correlation was tested used bivariate analysis (Pearson’s R as well as by multiple linear regression analysis. p values <0.05 were considered as statistically significant. Statistical analyses were performed using SPSS software Advanced Models 24 (IBM, Chicago, Illinois, US).

Population C

General Characteristics

Twenty-seven patients (12 males, mean age 69.4 ± 8, range 56-87), affected by metastatic NET, were included in the present analysis. Each patient underwent an FDG PET/CT and a 68Ga-DOTATOC PET/CT within a two-weeks period. At the moment of the first visit, blood pressure was measured, and a cardiovascular RF anamnesis was carried out. Cardiovascular risk stratification of the scanned patients was performed according to a simplified version of the Framingham model (including age, diabetes, smoking, systolic blood pressure BMI [48]. In particular, systolic blood pressure values, as well as treatment for hypertension were included in the Framingham score computation. Similarly, positive smoking history was considered in case of active smoking habit at the time of scan, as well as in case of past smoking habits. Finally, no information about severity of diabetes and/or to insulin or other treatment for diabetes was taken into account in the computation.

Exclusion criteria were the same as per the Population A.

Image Analysis

In all patients, a large VOI was constructed on the entire aorta, in both the FDG and in the 68Ga-DOTATOC PET/CTs. Here, SUVmean and SUVmax were computed. These values were then normalized for BP, to obtain TBRmax and TBRmean. TBRmean represented the overall mean uptake within the vessel wall while TBRmax was used to capture the highest activity, which was invariably located within the atherosclerotic plaque.

Statistical Analysis

All data are reported as Mean ± SD. Differences between groups were tested using one-way analysis of variance, with intergroup comparison afforded using Bonferroni test. Correlation was tested used bivariate analysis (Pearson's R as well as by multiple linear regression analysis). p values <0.05 were considered as statistically significant. Statistical analyses were performed using SPSS software Advanced Models 24 (IBM, Chicago, Illinois, US).

RESULTS

Population A

Arterial Plaques and whole aorta analysis

At the first PET/CT mean TBR within the vascular lesions was 2±0.8, while mean HU density and mean CS were 240±133 and 180±130. At the moment of the second PET, mean HU had increased up to 272±135 (p<0.001 Vs. the first PET) and CS had also increased to 220±274 (p<0.001 Vs. baseline). Mean TBR was not significantly changed. See Figure 3 for details.

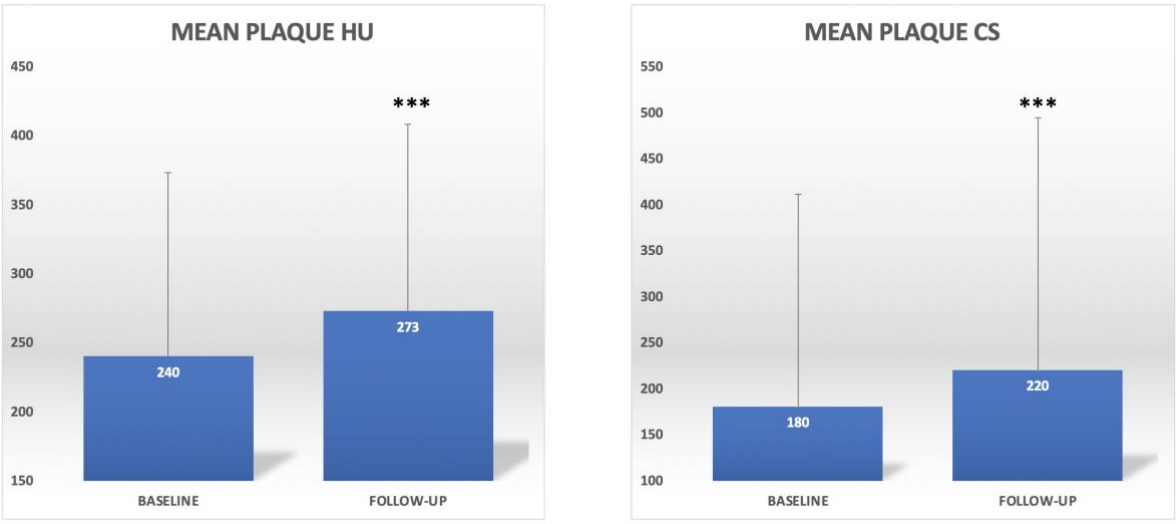

Figure 3. Values of mean HU density and Calcium Score. A significant increase can be highlighted at the follow-up PET. ***p<0.001.

Mean DHU% and mean DCS% were 19±20% and 51±59%, respectively; normalized values corresponded to 3±2% and 7±8%. A tight and direct correlation was noted between TBR in the plaques in the baseline PET and both NDHU% (R=0.67, p<0.01) and NDCS% (R=0,7, p<0.001), see Figure 4 for details.

An even stronger correlation was observed between mean TBR of the whole aorta and the total variation in CS in the entire vessel (R=0,85, p<0.001). See Figure 5.

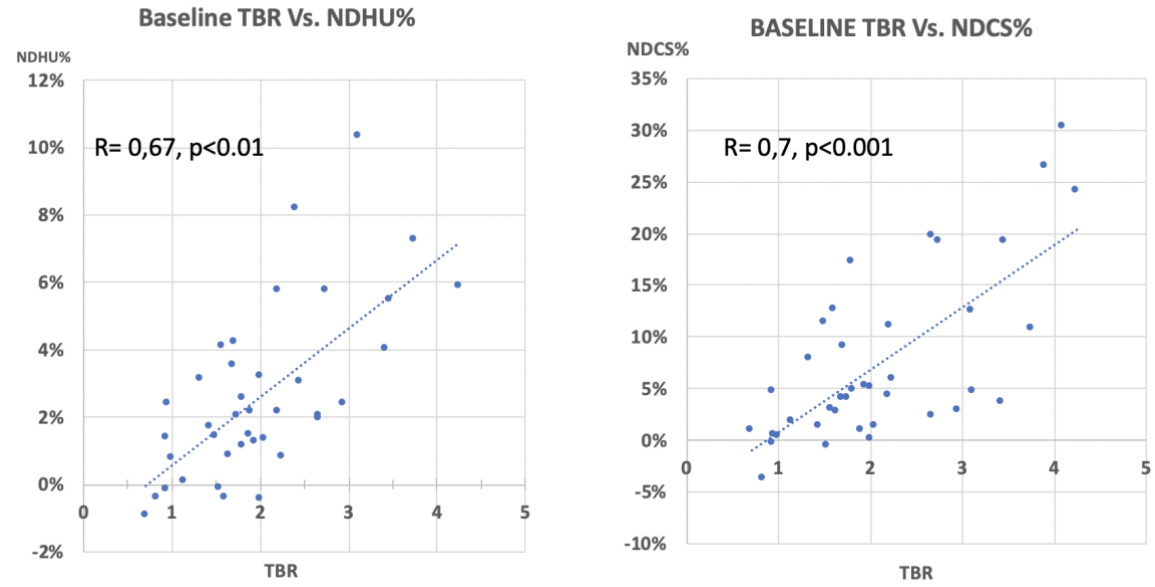

Figure 4. Correlation between baseline plaque TBR and calcification indices.

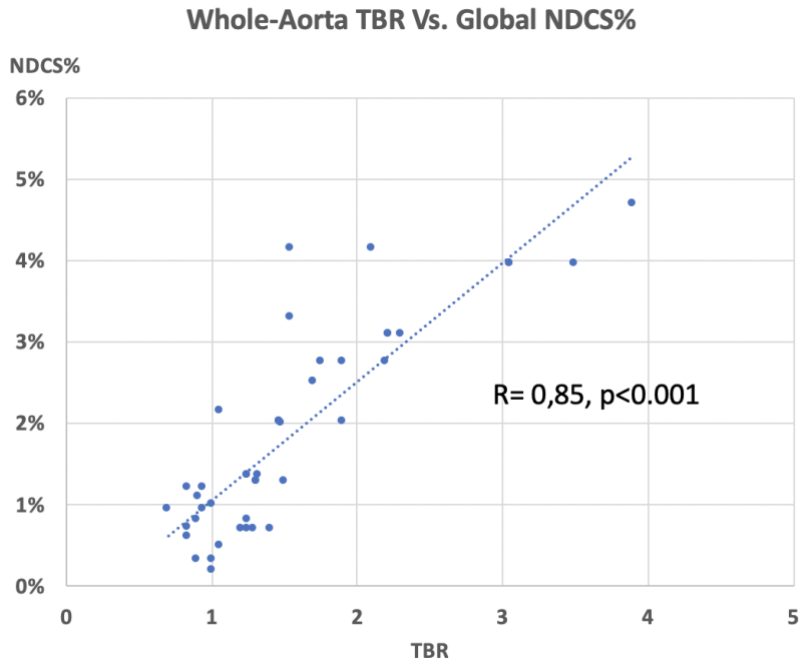

Figure 5. Correlation between baseline whole aorta TBR and total CS.

Gallery of representative plaques

Global plaque and aortic analysis showed that mean activity within the plaque predicted it future calcium content variation. Here, we highlight some representative cases where the activity of calcium deposition and the subsequent density variation were visible at PET/CT images qualitative observation.

Active and lightly calcified plaque

These plaques represent arterial calcium accumulation in their earlier stages. It is therefore common to observe a visible bone-seeking tracer accumulation within, as this phenomenon reflects the activity of the osteoblast-like cells residing within the plaque. Such lesions frequently present a significant variation of calcium content at follow-up. In Figure 6, an example of a very lightly calcified arterial wall is presented. At follow-up, activity within the atheromatous lesion hat diminished, but the calcium content has markedly increased.

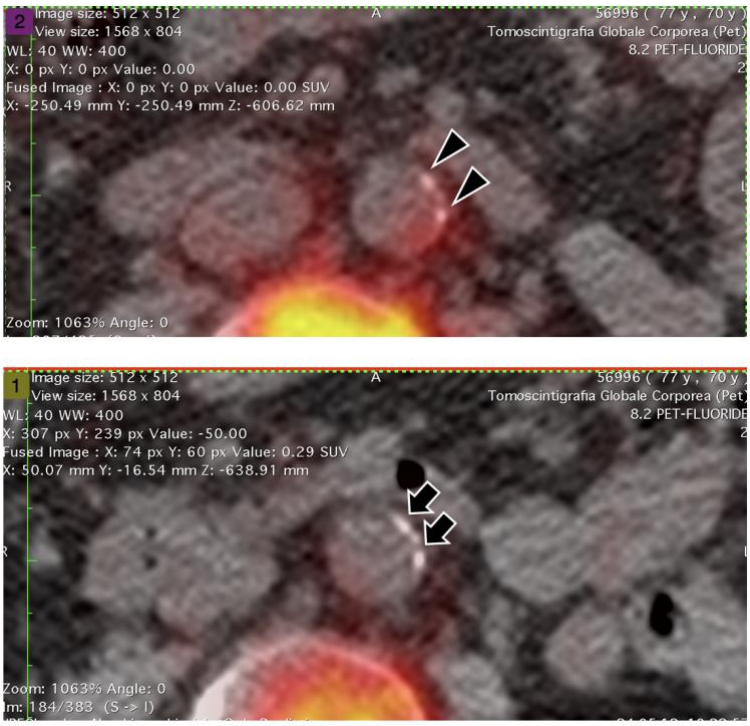

Figure 6. Early stage calcification, progressing at follow-up. At baseline (top panel) focal calcification cores, with moderate NaF uptake, are noted (arrowheads). At follow-up (bottom panel), tracer uptake has dwindled, but the calcification cores have expanded, and calcium density has markedly increased (arrows).

Mixed Plaque with actively growing segments

This kind of plaques represent a sort of intermediate stage between early, rapidly growing early plaque and the massive, old plaques, which are no longer actively concentrating calcium. Here we can see a multi-segment plaque, on its way to becoming a ring-shaped plaque, embracing the entire aortic wall. Here we observe some focal tracer uptakes, at the edge of major calcium chunks or between two bigger calcified areas. In the same regions, an increase in calcium content is observed in the follow-up images.

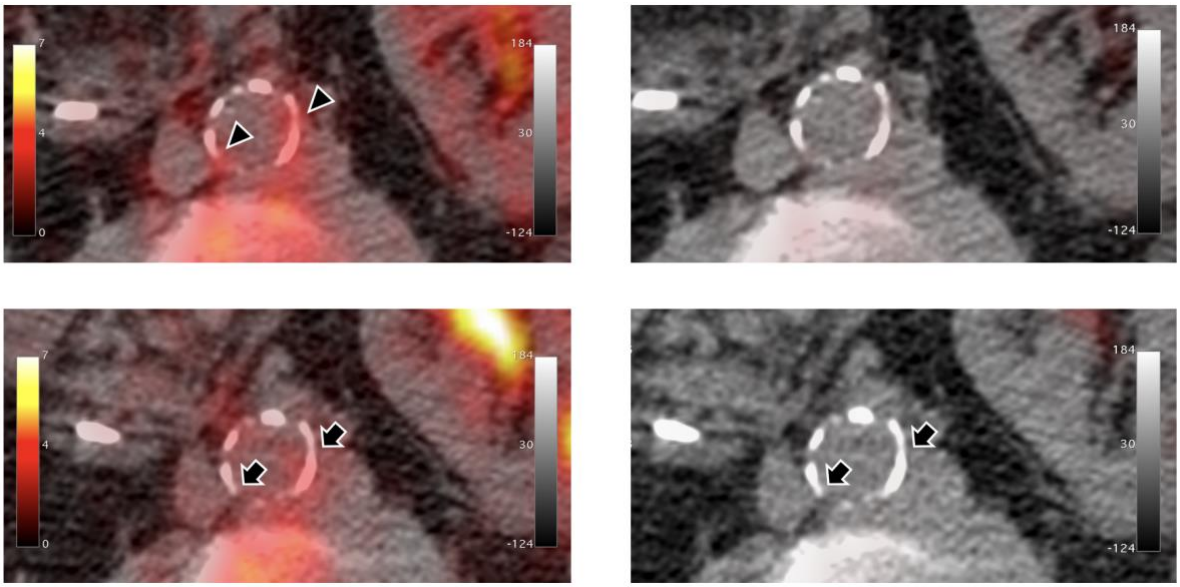

Figure 7. Mixed-type plaque. Notice the focal increased NaF uptake at the baseline PET (top left panel, arrowheads). In the same positions, increase in calcium content is observed and the gap between the two plaques on the left side of the aorta is closed (bottom left panel, arrows). The right panel show the CT images.

A plaque is born: significance of diffuse uptake

Non-calcified plaques are lesion that cannot be appreciated by morphological imaging. Their lack of calcium content and their lipid core imply a mean HU density which is near to that of vessel wall or of luminal blood. However, is some rare occasion, it is possible to capture the moment in which a calcified plaque is “born”. In fact, non-calcified lesions represent the earlier stages of atheromatosis’ evolution. As described, the chronic inflammation fosters a

commitment of the mesenchymal cells to the osteoblast line. These bone-forming cells then start concentrating and laying calcium onto the plaque. This activity can be registered by NaF-PET, either as focal or diffuse tracer uptake within the vascular wall. On follow-up scans, it might be possible to witness early cores of calcification, which will then build up the early calcified plaque.

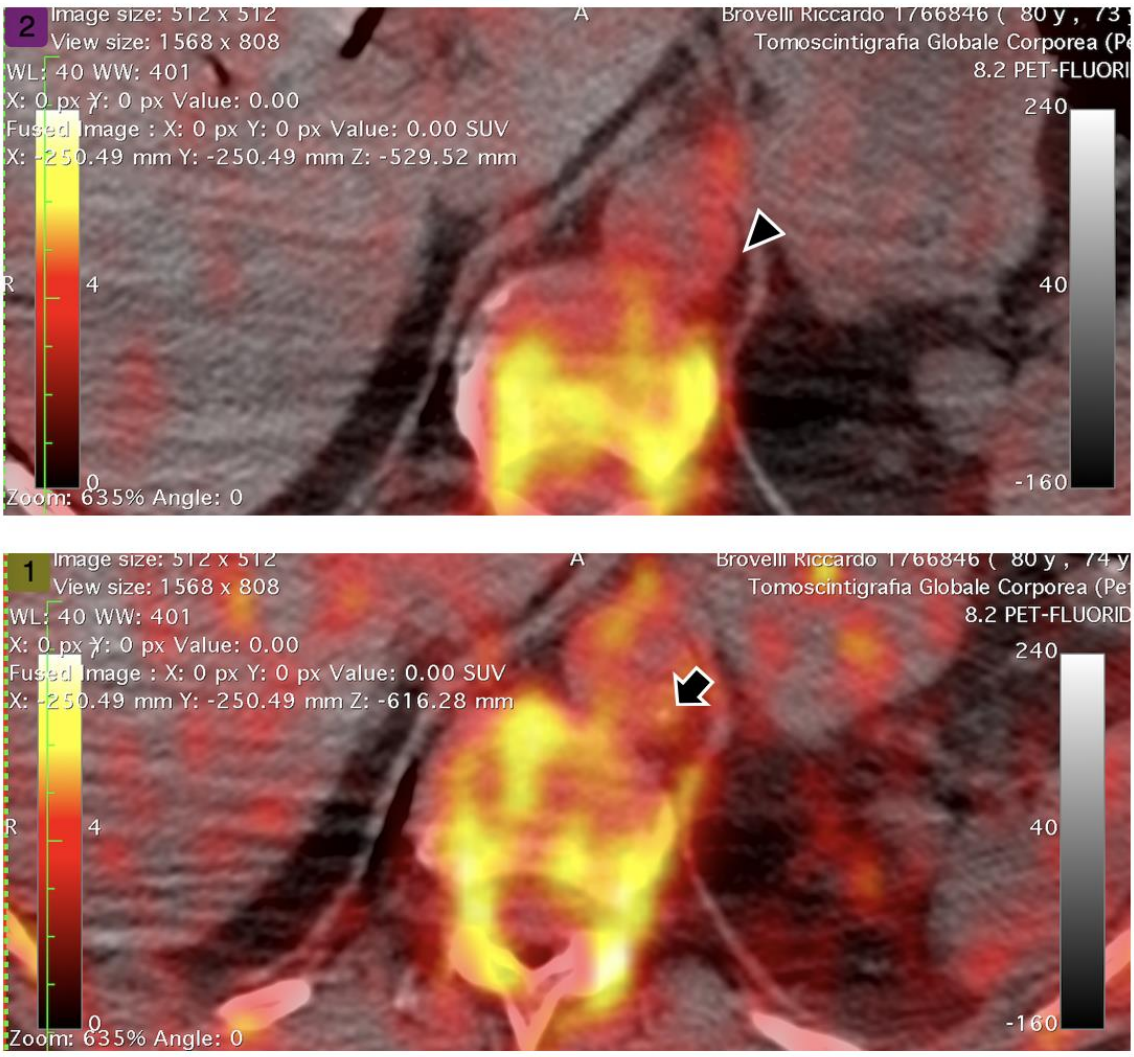

Figure 8. Birth of a calcific plaque. In the baseline fusion images (top panel), a mild NaF uptake is observed, which delineates the entire left and posterior sides of the abdominal aorta. On the follow-up PET/CT, the tracer uptake became much more intensive and diffuse, affecting the whole vessels circumference. A lightly calcified spot is now observed posteriorly left (bottom panel, arrow). In retrospect, a tiny calcified spot may be observed in the baseline scan (arrowhead), however, this bit of calcium is not picked up by the algorithm, as it doesn't reach the 90 HU mark.

Heavily calcified plaques

This entity is the last stage of arterial calcification. In these plaques, no uptake is observed and no significant variation between baseline and follow-up can be demonstrated (data not shown). These lesions tend to display HU values averaging near the upper limit of the scale and close to the one of compact bone; the encase the whole arterial volume and stretch for numerous CT slices.

POPULATION B

Characteristics of the study population

Out of the 79 study patients, 60 (76%) had evidence of bone localizations while 19 (24%) had no highlightable metastases. Table 1 lists the main characteristics of the study population, including a comparison of patients with and without bone metastases. The prevalence of major cardiovascular risk factors and medications did not differ between these groups, except for a slightly higher prevalence of diabetes in those without bone metastases (50% vs. 21% in those with metastases, p=0.03). The only significant difference in ^{18}F-NaF PET/CT-derived parameters was a higher aortic mean HU in those patients with evidence of bone metastases (241.8±58.7 vs. 241.8±58.7 in those without metastases, p=0.03). There were no other differences in bone-related parameters.

On the basis of the tercile stratification, the "heavy" and "medium" calcifications' groups counted 26 patients each and the remaining 27 patients were placed in the "light" calcification group.

Table 1. Clinical characteristics of the population B.
WB: Whole-body.

CLINICAL VARIABLES	All Patients with Plaques N=79	No metastases N=19	Evidence of Metastases N=60	Controls N=35	P value (Metastases Vs. no Metastases)	P value (Patients Vs. Controls)
Age, years	70.8 ±8.04	70.5 ±10.5	70.9 ±7.17	72.4 ±6.1	NS	NS
Women	65%	89%	57%	45%	0.009	NS
Previous chemotherapy	41%	11%	51%	62%	0.002	0.045
Previous radiotherapy	55%	32%	63%	65%	0.02	NS
Previous chemo- or radiotherapy	63%	32%	73%	81%	0.001	0.039
Previous chemo- and radiotherapy	29%	11%	35%	43%	0.04	NS
Body mass index, kg/m^2	25.3 ±4.6	26.9 ±3.6	24.8 ±4.8	23.2 ±2.8	NS	NS

Obese (body mass index≥30 kg/m^2)	9%	16%	7%	6%	NS	NS
Smoking history	58%	57%	58%	N/A	NS	-
Hypertension	67%	69%	65%	N/A	NS	-
Antihypertensive medications	66%	77%	61%	N/A	NS	-
Dyslipidemia	46%	43%	47%	N/A	NS	-
Lipid-lowering medications	25%	31%	24%	N/A	NS	-
Diabetes	29%	50%	21%	N/A	0.03	-
Bisphosphonates	7%	0%	7%	N/A	NS	-
Warfarin	7%	0%	7%	N/A	NS	-
Proton pump inhibitors	31%	29%	31%	N/A	NS	-

Uptake and calcification Indices

In patients with ACs, mean TBR in the trabecular bone was 6.2±3.9 and mean trabecular bone density was 137±25 HU. The mean TBR of all aortic plaques was 1.9±1.2, with a mean HU density of 227±61. Control patients without ACs had a markedly higher vertebral density (160±14 HU, $p<0.001$ Vs. patients with plaques) and a slightly higher mineral metabolism (TBR 8.4±3.4, $p<0.05$ vs patients with plaques). Among the patients with ACs, a progressive reduction in mineral metabolism as well as in trabecular bone density can be observed when comparing the three subgroups, whereas patients with "heavy" calcifications show significantly reduced values in comparison with these with "light" arterial calcium deposits.

In fact, mean trabecular TBR values were 8.3±4, 4.5±2,1 and 3.5±1.8 in light, medium and heavy calcifications' groups, respectively ($p<0.05$ for light Vs. medium and $p<0.01$ for light Vs. heavy). Similarly, mean trabecular HU was 143±19, 127±26 and 119±18 in the three groups, respectively ($p<0.01$ for light Vs. heavy). Finally, uptake intensity within the plaque dwindled when progressing from heavy to light calcifications (TBR:

2.1±1; 1.8±1 and 1.4±0,6 for light, medium and heavy calcifications, respectively, $p<0.05$ for medium Vs. heavy and $p<0.01$ for light Vs. heavy).

See Figure 9-10 and Table 2 for details.

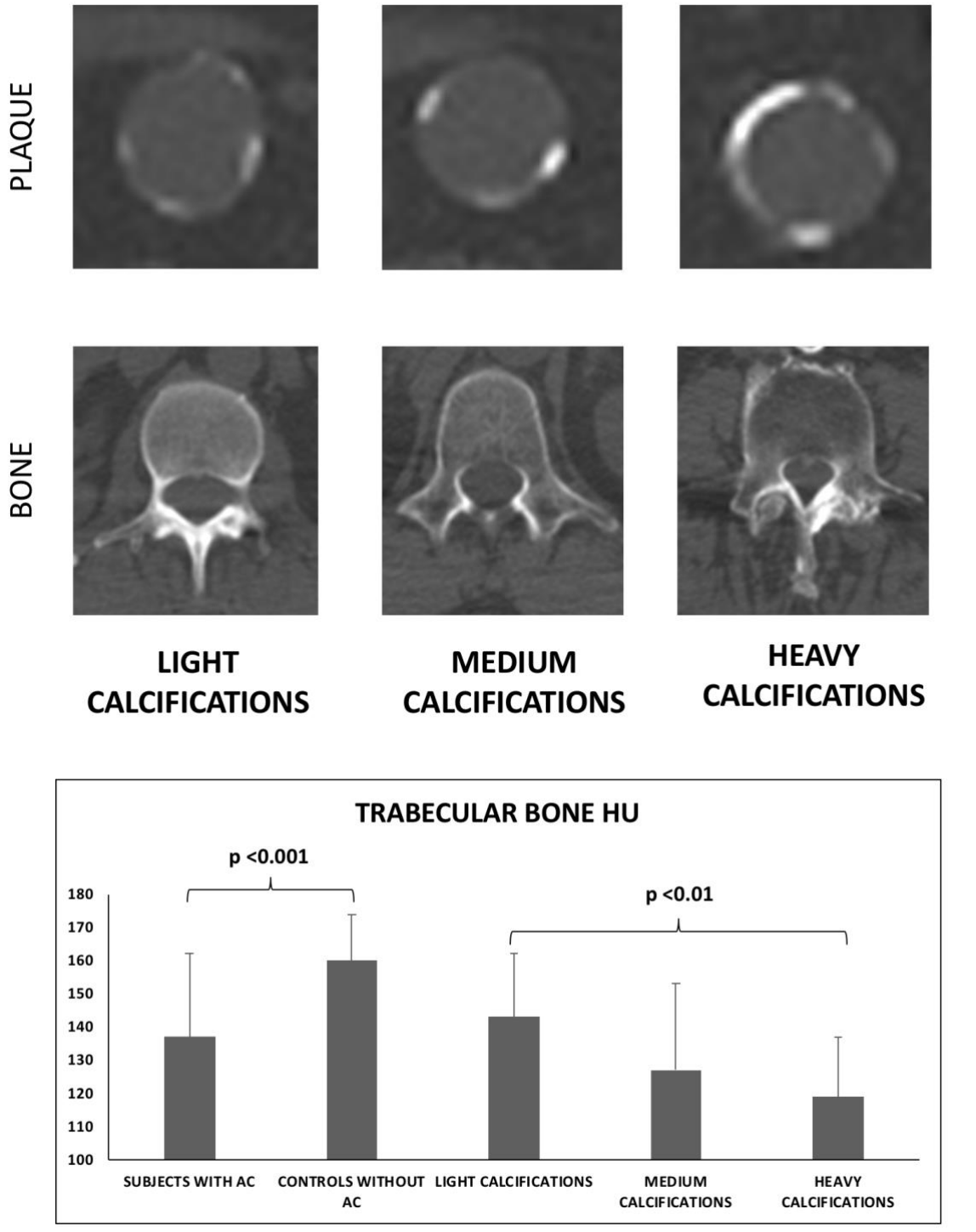

Figure 9. Density trabecular bone and in the aortic plaque. In the three top panels are displayed low-dose CT images depicting examples of typical "light", "medium" and "heavy" plaques. Directly below (middle panels) are displayed CT slices of the trabecular bone from the same patients.

After terciles stratification according to mean plaque density, subjects with a higher mean plaque thickness presented a decreased vertebral density and metabolism (lower histogram).

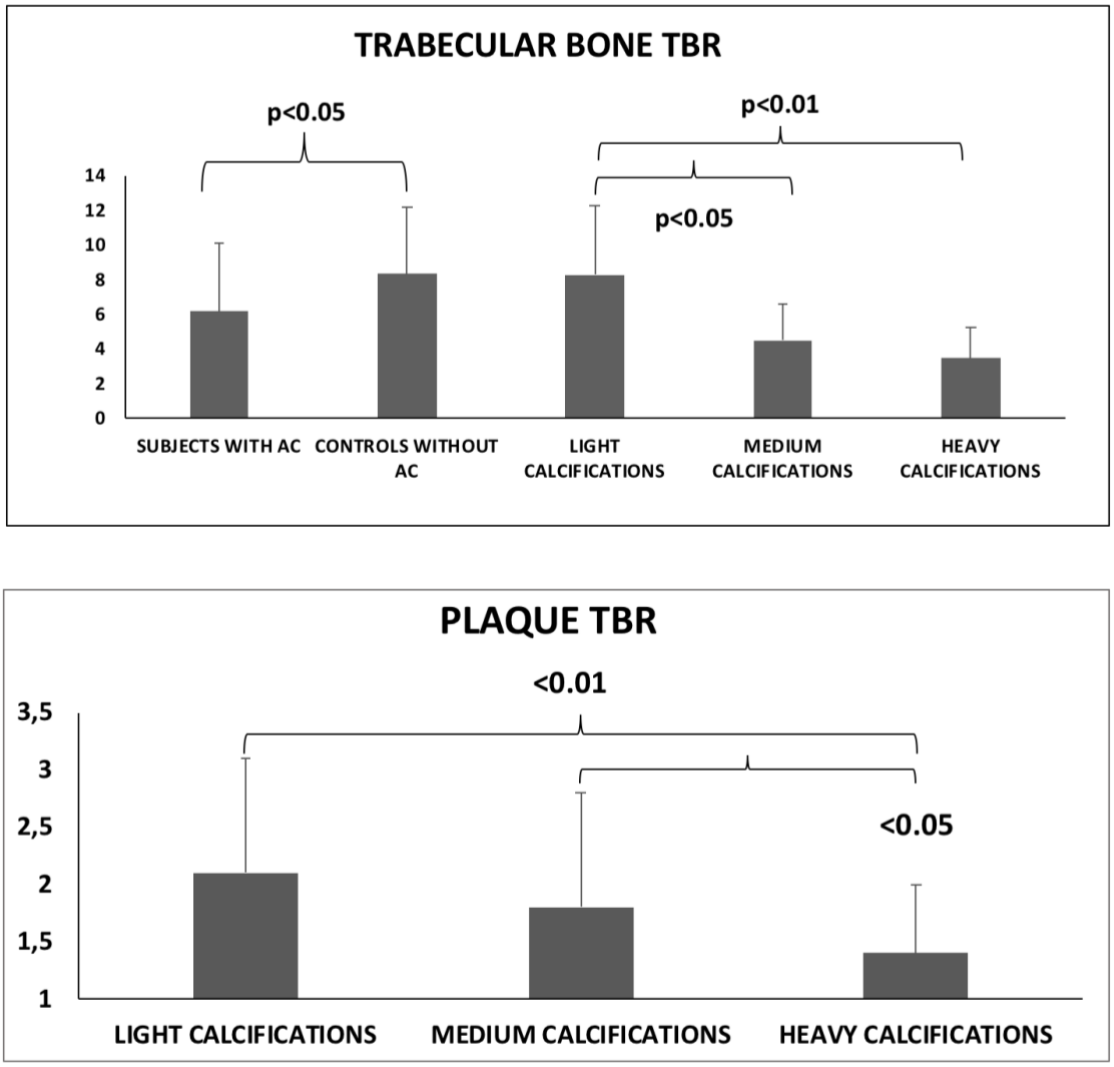

Figure 10. Mineral metabolic activity in patients and controls. The histograms depict the target-to-background ratio of subjects with a ACs and of controls in trabecular bone (upper) and the corresponding value within the plaques. Subjects with ACs had a lower TBR than controls; however, this metabolic decrease was circumscribed to patients with medium and heavy calcifications. Likewise, plaque TBR was higher in less heavily calcified plaques.

Table 2. Radiological characteristics of the patients' population.

^{18}F-NaF PET/CT VARIABLES	All Cases with Plaques N=79	Group I: No metastases N=19	Group II: Metastases N=60	Controls without plaques N=35	P value (Group I Vs. Group II)	P Value (Plaques Vs. Controls)
BONE VARIABLES						

Bone mean HU	137±25	135±31	126±18	160.3±14	NS	<0.001
Bone mean TBR	6.2 ±3.9	5.9 ±2	6.4 ±4.5	8.4 ±3.8	NS	0.034
AORTIC PLAQUE VARIABLES						
Aortic mean HU	227±71	206±65	245±59	-	0.026	-
Aortic mean TBR	1.9 ±1.2	1.9 ±1.4	2 ±1.1	-	NS	-
Infrarenal aortic diameter, mm	18.6 ±4.4	18.1 ±1.6	18.8 ±4.9	-	NS	-

Interaction between plaque and bone

Mean plaque density showed an inverse association with vertebral HU density (R=-0.56, p<0.01, Figure 11). In opposition, no correlation between age and HU density was observed. Conversely, plaque and trabecular bone TBR were directly and closely correlated (R=0.63 and p<0.001, Figure 11).

Arterial plaque HU density displayed an inverse correlation with its own TBR (R= -0.42, p<0.05, Figure 12), as well as with lumbar vertebrae TBR (R= -0.47, p<0.01, Figure 12).

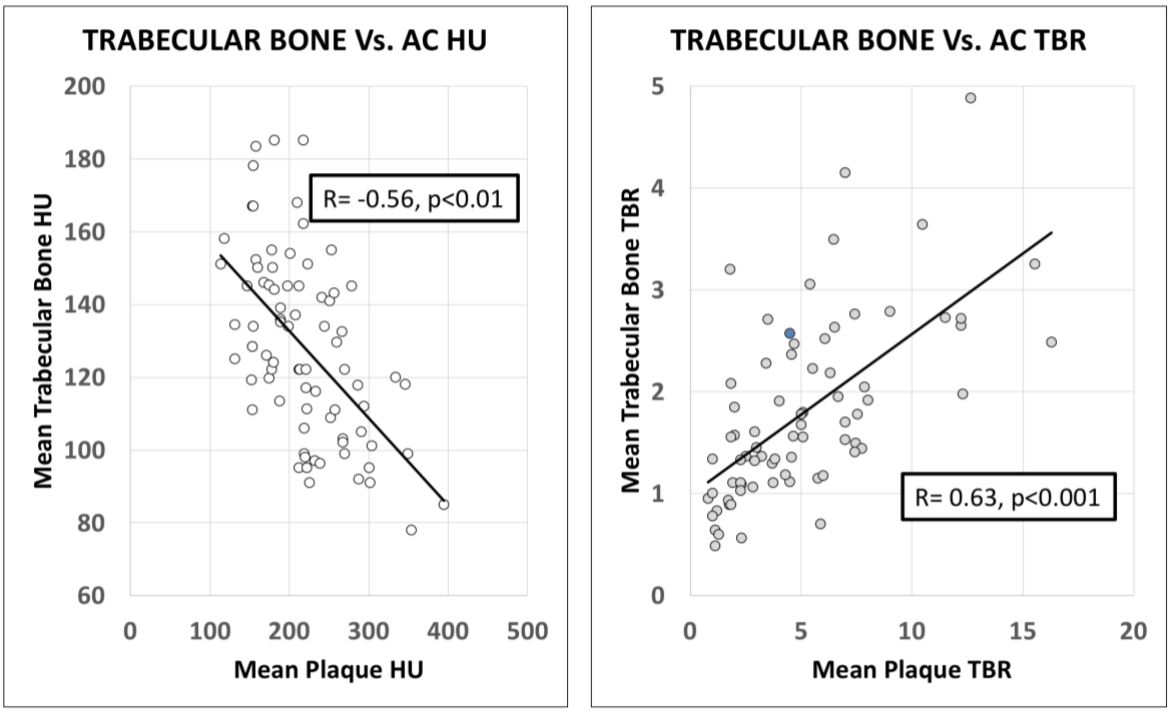

Figure 11. Correlation between vertebral density and plaque features. A higher plaque density was associated to a lower trabecular density; conversely, TBR in the AC was directly associated with the one in the trabecular skeleton.

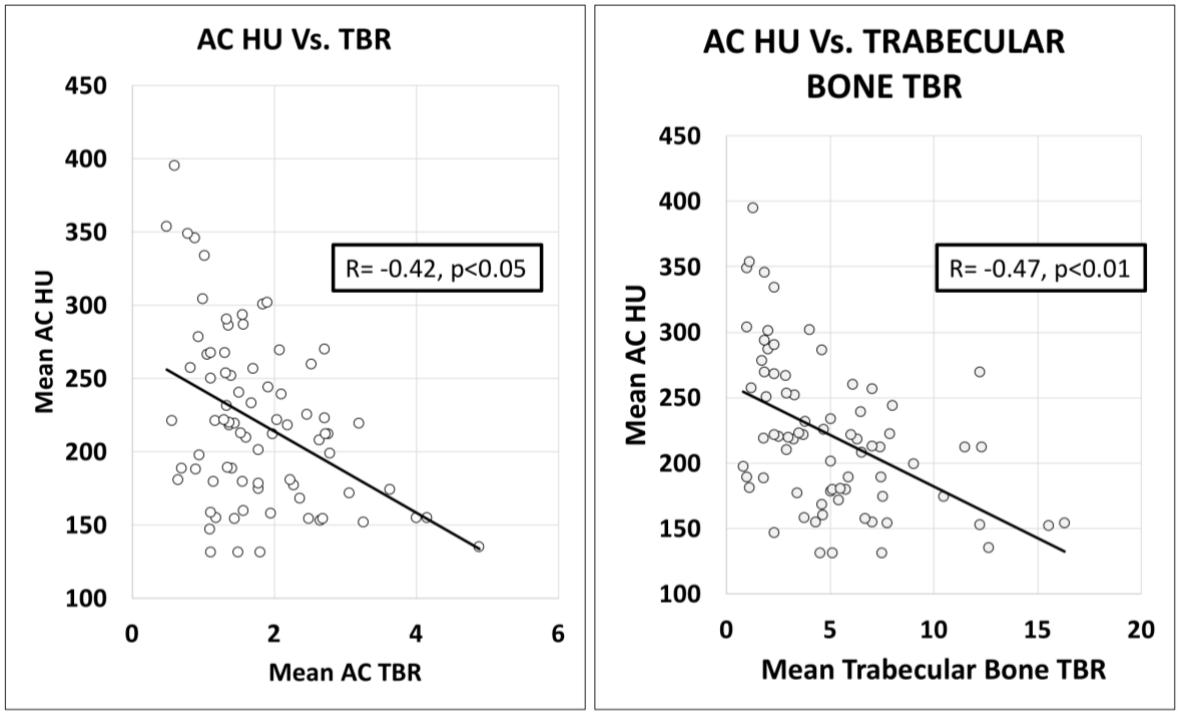

Figure 12. Correlation between plaque and trabecular mineral metabolism. Patients with thicker arterial calcifications showed a reduced mineral metabolism within the plaque itself and in the trabecular bone.

Multiple regression analysis of plaque density and metabolism

At univariate analysis, mean HU density of aortic plaque was not predicted by any of the cardiovascular risk factor or by age; conversely, it was related to its own TBR (p=<0.001) as well as by trabecular bone TBR (see Table 3 for details). Mean vertebral density was related only to plaque density (p<0.05); conversely age, use of bisphosphonates and previous radio/chemotherapy had no influence on vertebral status (Table 4).

Table 3: Multiple Regression Analysis of Parameter affecting aortic plaque density (HU)

	Standardized Coefficient			95% Confidence Interval	
Variable	Beta	t	Sig.	Lower Bound	Upper Bound
Age	0.168	1.503	NS	-0.407	2.91
Gender	-0.033	-0.296	NS	-32.12	23.813
Smoking History	-0.108	-0.929	NS	-29.935	10.896
Hypertension	0.032	0.271	NS	-23.938	31.486

Diabetes	0.025	0.21	NS	-28.048	34.648
Dyslipidaemia	0.061	0.51	NS	-20.355	34.339
Aortic Plaques TBR	-0.401	-3.786	<0.001	-43.009	-13.351
Mean trabecular TBR	-0.558	-3.863	<0.001	-14.966	-4.641

Table 4: Multiple Regression Analysis of Parameter influencing Vertebral Density (HU)

Variable	Beta	t	Sig.	95% Confidence Interval for B	
				Lower Bound	Upper Bound
Chemotherapy	-.154	-.685	NS	-31.308	16.077
Radiotherapy	.370	1.658	NS	-4.738	37.925
Bisphosphonates	-.215	-1.188	NS	-68.115	19.372
BMI	.342	1.643	NS	-.711	5.489
Age	-.045	-.220	NS	-1.419	1.154
Gender	.247	1.15	NS	-0.856	1.152
AC Density (HU)	-.546	-2.671	.014	-.398	-.051
Mean trabecular TBR	-.050	-.214	NS	-3.347	2.737
Mean AC TBR	-.105	-.331	NS	-22.264	16.278

POPULATION C

General Population characteristics

On average, the cardiovascular risk score was 12,5±9,1% (range 2,1% - 35,7%). Among the 27 patients 11 (41%) were classified as having a low CV risk (30-years MACE-likelihood <10%), 10 (37%) were at medium risk (MACE risk between 10% and 20%) and six (22%) presented a high CV risk (acute events likelihood >20%).

Mean systolic blood pressure was 135±23 mmHg and 22 subjects (81%) were on antihypertensive medications. Mean BMI was 29,2±5,6. Eight patients (29%) were active smokers at the time of the first visit. Twelve patients (44%) suffered from diabetes mellitus (DM).

Uptake value of FDG and SSR-tracer

Average TBRmean was not significantly different between FDG and 68Ga-DOTATOC (1,2±0,5 Vs. 0,8±0,6, respectively p= ns). Conversely, the mean of TBRmax was significantly higher in 68Ga-DOTATOC PET, when compared to FDG (5,7±3,1 Vs. 2±1,2, $p<0.01$). See Figure 13 for details.

A tight and direct correlation was noted between FDG TBRmean and CV risk score ($R=0.82$, $p<0.001$), as well as between 68Ga-DOTATOC TBRmean and CV risk score ($R=0.81$, $p<0.001$). See Figure 14.

Finally, average TBRmax of FDG was not significantly different when considering patients with DM versus the remaining ones (2.1±0.5 Vs. 1.8±0.4, p=ns); however, TBRmax of 68Ga-DOTATOC was slightly higher in DM patients when compared to the non-diabetic ones (6±2.1 Vs. 4,9±0,9, $p<0.05$). Details are to be found in Figure 15.

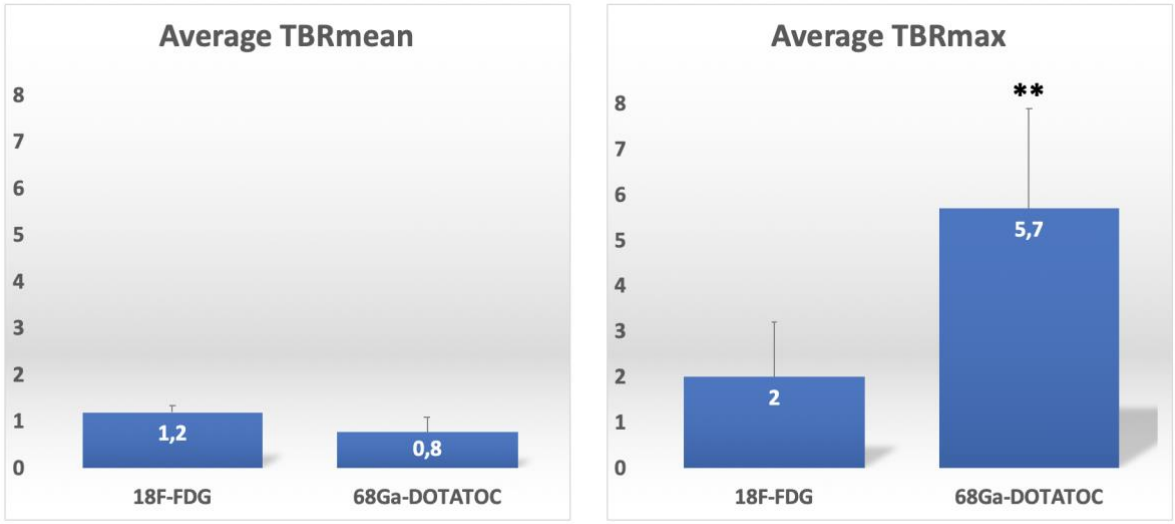

Figure 13. Average uptake within the vascular VOI. **p<0.01

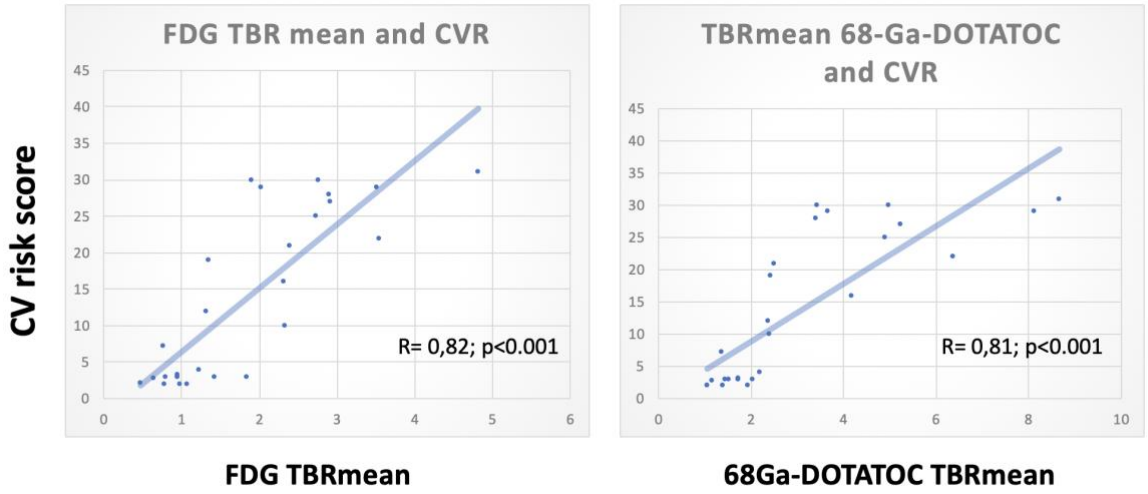

Figure 14. Correlation between mean vascular uptake and CV risk score.

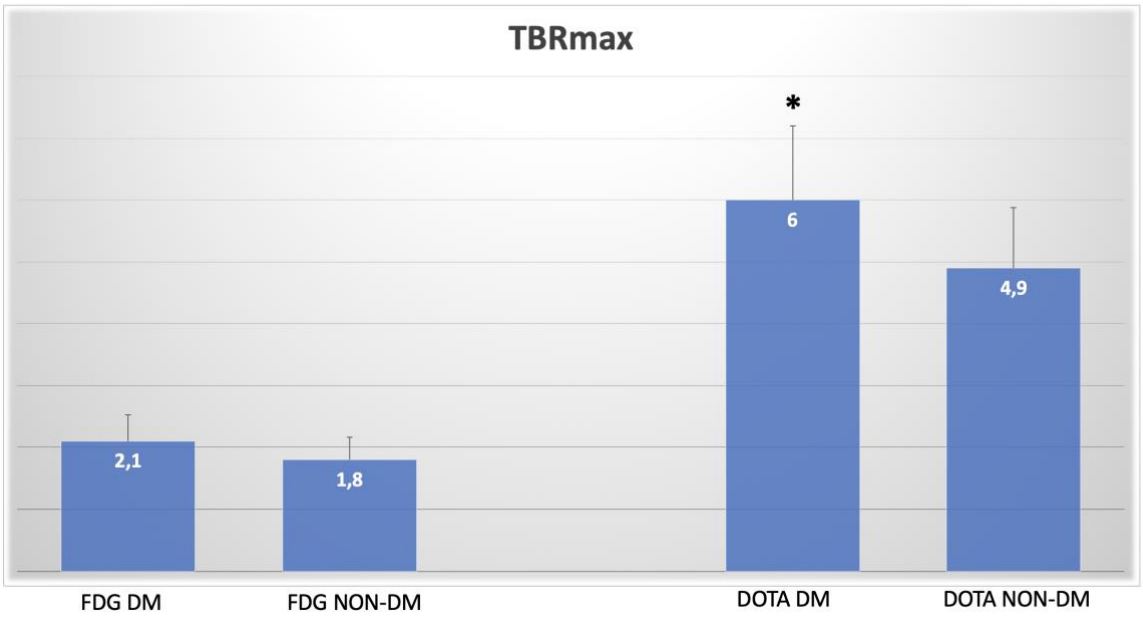

Figure 15. Uptake in diabetics and non-diabetics. *p<0.05

Gallery of representative plaques

FDG-positive, 68Ga-DOTATOC-negative plaques

FDG uptake is a common finding in growing arterial calcifications. Such an increased tracer distribution is prevalently observed within plaques presenting a very thin calcification, like the one displayed in Figure 16. Here, we can observe a diffuse FDG activity, which is diffused within the entire calcification ring, and a very faint SSR-tracer uptake, which localizes predominantly in the thinner posterior segments.

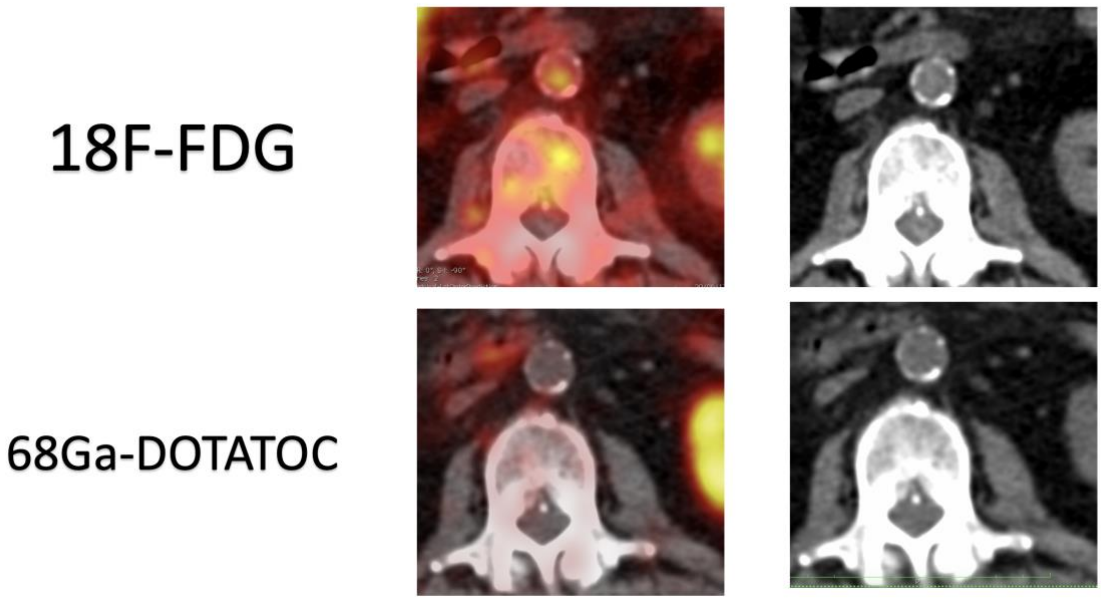

Figure 16. FDG-positive (upper panels), SSR-tracer negative (lower panels) arterial plaque.

68Ga-DOTATOC-positive, FDG-negative plaques

This type of plaque presents an intensive (often focal) somatostatin-receptor tracer uptake while displaying no visible glucose metabolism. Comparably to the FDG-positive plaques, these arterial calcifications are thin and mildly dense in nature; an example of such plaque can be seen in Figure 17. Here, a mild FDG uptake can be observed in the right-side plaques.

However, the focal 68Ga-DOTATOC uptake, which is observed in the right-posterior plaque, present a markedly higher tracer intensity.

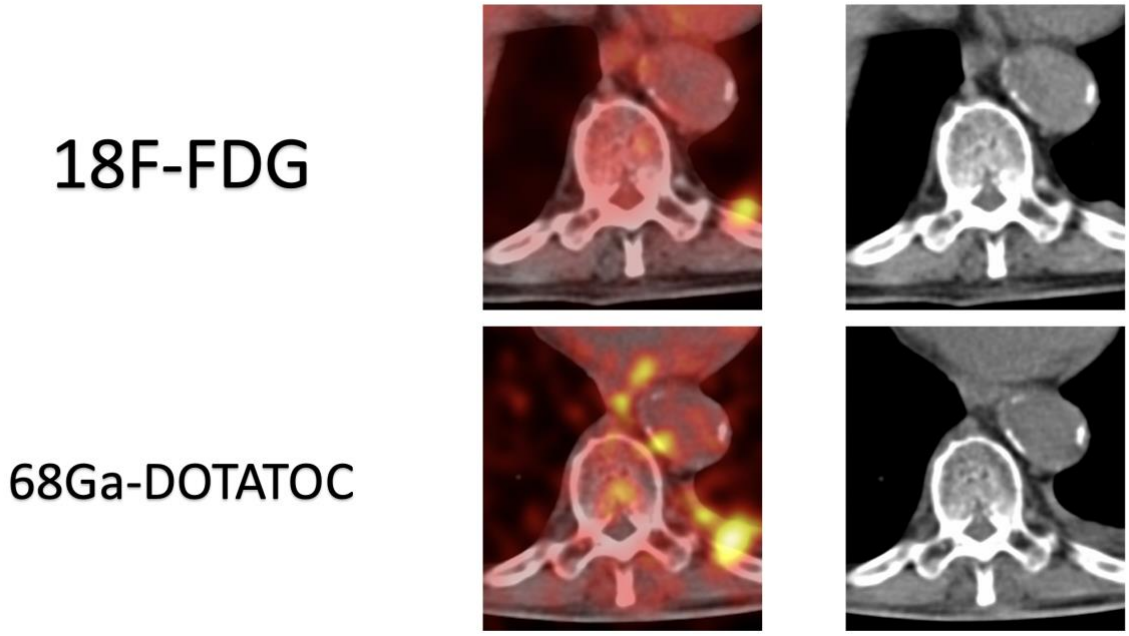

Figure 17. FDG-negative (upper panels), Ga-DOTATOC-positive (lower panels) plaque.

Tracer-negative plaques

In opposition to the above-described cases, some plaques might present neither FDG nor SSR-tracer uptake. In most cases, such arterial calcifications are in a very advanced stage and present a high attenuation value. As discussed, a tracer substance can be trapped within a tissue only in the presence of an adequate cellularity or of active metabolism caused by ongoing processes. End-stage calcifications do not display these features. However, they could progress over time, owing to passive calcification mechanisms such as calcium salt precipitation in the presence of damaged endothelium.

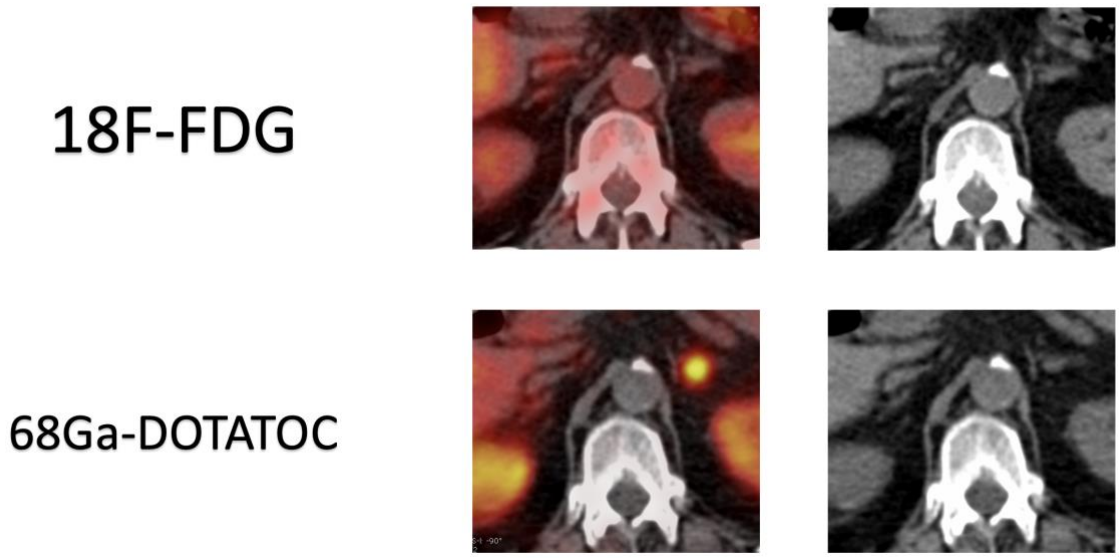

Figure 18. Advanced plaque, not showing any tracer uptake.

DISCUSSION

The present work reports the analysis of plaque metabolism, conducted used three of the most widely available PET radiotracers and aimed at determining the significance of radiopharmaceutical uptake within the calcified lesion. Our results show that sodium fluoride uptake, tracing osteoblast activity within the atherosclerotic microenvironment, is a marker of subsequent evolution of the plaque calcium content. Moreover, we have shown that both glucose metabolism and density of somatostatin receptors within vessel walls are linked to cardiovascular risk, however, SSR2 imaging might be apter in capturing the plaque inflammation in diabetic patients.

In the following paragraphs, we are going to discuss these results in light of the existing literature evidence. Moreover, we will try to analyze the possible future direction of the plaque imaging research.

Fluoride PET: a key to understanding the plaque mineral turnover mechanisms

^{18}F-Sodium fluoride represents the most ancient PET tracer [49]. First introduced in the sixties, it was later dropped for 99Tc-based agents, which featured lower costs and a more favorable absorbed-dose profile [50]. The relatively recent introduction of hybrid PET/CT scanners contributed to re-awakening the interest in this tracer, which presents a higher sensitivity when compared to single-photon bone-seeking agents [51]. Recent progress in the PET technique, including 3D acquisition, time-of-flight photon origin detection, point spread function, and others, enable the characterization of smaller structures, such as the atherosclerotic plaque [41]. To this point, research on the field has been pointed in characterizing the uptake patterns within the plaque or within the vessels [33; 45; 52] or in defining the culprit plaque after an acute event [46]. In particular, coronary plaques that

have undergone rupture and that have caused myocardial infarction, present an increased fluoride uptake. This feature is not surprising, as the acute inflammation and the reparative process foster an increased mineral metabolism in the area. More interestingly, the authors have found a correlation between high-risk plaque characteristics in patients with stable angina and radioactive tracer uptake, a result that was also confirmed by further studies [53]. However, it is not known whether patients with stable angina and NaF-positive plaques did present acute infarction in their subsequent clinical history. It might be as well possible that the uptake was caused by continuous calcium deposition within the growing plaque, which in turn caused the clinical symptoms. As it is, there are not enough data to be able to recommend an invasive procedure, having the purpose of preventing later cardiovascular events, in patients with elevated fluoride uptake within a coronary plaque.

For these reasons, in the current work, we focused on the slow-and-steady nature of plaque growth. If the atherosclerosis is a process that spans over decades, it might make sense to check scans that are spaced months or years apart, to see if anything changes. Our results confirm the hypothesis of slow growth of the plaques: this phenomenon was observed mainly in those lesions with high sodium fluoride uptake and correlated with the intensity of tracer accumulation.

Similar results have been reported by Dweck and colleagues, who detected a tight positive correlation between fluoride uptake and an increase of calcium score in a segment affected by aortic stenosis [54]. Interestingly, after removing from the computation those plaques, which presented a more-advanced calcification pattern, the correlation gained further significance. This finding supports the hypothesis that NaF-PET should be directed in analyzing the early-stage calcification, showing active deposition mechanisms. In another study by Li and colleagues, a trend towards calcification increase was found, which was

associated with increasing NaF and decreasing FDG uptake: these data could support the hypothesis that inflammation is prevalent in the earliest, non-calcified plaque phases, while increased mineral turnover prevails later on [55]. Ishiwata and co-workers found an association between background-corrected fluoride uptake and the increase of both volume and calcification score of arterial plaques [56]. They did not however identify a correlation between tracer uptake and HU variation. However, they had a smaller population and they did not correct for the time elapsed between the two scans: this point is relevant, as a greater increase of calcium is expected when more month since the baseline scans have elapsed. Furthermore, they work analyzed the link between focal NaF accumulation and appearance of calcium in follow up scans: this was the case in about one-fifth of the cases. It must be considered that their study population also included non-oncologic patients, who presumably received a lower tracer activity and who could have been younger than the rest of the population. Moreover, a mean follow-up of one year might be insufficient to witness visible calcification in the hot spot area. A HU analysis of the region might have served this purpose.

Overall, existing literature is currently not plentiful, yet it hints towards a major role of fluoride accumulation in predicting subsequent plaque evolution. The relative inconsistency of some results might be caused by the generally small sizes of the examined samples and by the difference in methodology. However, almost all authors have applied some sort of background correction, which led to reproducible results in term of target-to-background ratios across all studies. On the other hand, follow-up studies were carried out at different intervals. This is understandable, given that the execution of PET/CT has always been driven by clinical need and prospective studies with ethical clearance to apply a radioactive substance to patients without recognized Fluoride-PET indication are non-existent. However,

time normalization should always be applied. Also, plaque density should be measured with a recognized algorithm in all cases (i.e. the Agaston score), so as to account for plaque volume and density the at the same time.

The interaction between bone and plaque: a new window into atherosclerosis' pathophysiology?

The existence of a link between atherosclerosis' progression and bone was first postulated on the basis of the observation that subjects with massive arterial calcifications also showed a high prevalence of osteoporosis [57; 58]. However, this was considered mostly a coincidence, as both conditions are fairly common in advanced age. However, our data showed that an inverse correlation between calcification density and mean trabecular bone HU exists and that age does not play a relevant role in this association. Moreover, fluoride activity within the bone, which mirrors the density and the activity of the bone-forming matrix, is reduced in patients with plaques compared to those without plaques, and it is further reduced in those bearing "heavy" calcifications. Two consequences may be inferred from this observation: that patients with arterial calcifications should be screened, and eventually treated, for osteoporosis; and that observing the bone matrix could grant an easy-access window onto the atheromatosis' pathophysiology. Since we have a number of effective treatments against osteoporosis, it might be conceivable that such medications could be effective against plaque progression as well. This hypothesis has been to this date barely investigated: the only available data originate from a subpopulation of the FREEDOM study, where the effect of a long-lasting Denosumab (specific RANKL-antibody) therapy on CV risk and calcification progression were tested against placebo [59]. The study failed to demonstrate a CV benefit of the drug over a three-year period (a non-significant 2% risk

reduction of cardiovascular events was observed). However, this study included only female patients, with 91% of patients being older than 70 years. Moreover, the follow-up period was limited to three years. Therefore, it is unknown whether this approach would be effective if applied to the male gender, if started at an earlier age or if its effects are evaluated with a more extended follow-up. In fact, considering the long-term course of the atherosclerotic disease, a continuous treatment might be in order to achieve full effect. Even if the anti-resorption therapy should prove unsuccessful in delimiting plaque growth, it could nonetheless be used to prevent bone loss and consequently to limit the fracture risk in these patients.

Comparing these data to the existing literature is challenging, for they are based on an in-house built software application, which has been specifically designed for the scope of isolating the signal originating from the trabecular bone. As a matter of fact, a decreased HU density within the trabecular bone is a common finding in patients suffering from oncological disorders such as CLL, multiple myeloma and metastatic castration-resistant prostate cancer [60-62]. However, bone HU density was significantly different among the different plaque thickness groups, while no differences were observed between patients with metastatic and non-metastatic disease.

In conclusion, these data confirm that arterial is not an isolated epiphenomenon of plaque progression within the arterial wall, but instead might involve and affect multiple systems, among which trabecular bone, as the main calcium storage of the human body, might play a prominent role.

Detecting plaque inflammation: going sure-fire or going specific

Our data, in keeping with those of the existing literature, demonstrated a direct correlation between FDG and SSR-tracer uptake and estimated cardiovascular risk [63]. This is explained by the fact that the presence of risk factors promotes atherosclerosis, which is in turn associated with inflammation, which is picked up by glucose metabolism or SSR imaging. However, arterial hotspots were more easily detected by 68Ga-DOTATOC rather than by FDG imaging. This phenomenon depends on the different specificity of the two imaging techniques: while FDG uptake might be moderately increased in almost any kind of inflammation-related cell, SSR2 are only expressed on the surface of activated macrophages [38]. Moreover, we demonstrated a higher 68Ga-DOTATOC uptake in diabetic patients: this is probably caused by the insulin-resistance mechanisms, which inhibit GLUT expression and cause an increase of circulating glucose, which then competes with FDG for tissue uptake. It follows that, when inflammation is to be tracked, 68Ga-DOTATOC should be the tracer of choice. On the other hand, FDG might be employed in those centers that do not perform SSR imaging on a regular basis.

A glance into the future

Using PET-based tracer could have a number of applications in patients suffering from atherosclerosis. Thanks to the dual morphological and functional nature of PET/CT imaging, it would be conceivable to employ a whole-arterial or aimed examination (e.g. on the coronary district) to assess the extension, the density and the metabolism of the atherosclerotic disease. In this setting reducing the tracer activity and employing low-dose CT protocols could contribute to reducing the absorbed dose. It would be then possible to track the development of the disease by performing serial examinations. The compliance of

the patient could be tested by using this method. In fact, it could be synergic in offering additional motivation (for instance in BMI reduction, or in meeting the blood pressure and glycemia goals) in high-risk patients. In fact, the patient would not solely be aware of the improvement of the clinical score (BMI, blood sugar and so on) but he or she could potentially see on the radiological monitor his or her own arterial plaque losing “steam” as the risk-reduction strategy kicks in. Should the patient suffer a MACE, it would be possible to analyze the coronary plaque status retrospectively, allowing, over time, to build up a database of high-risk plaques, which could allow in pre-empting such events. New computational application, namely machine learning and AI, could read these data and learn to recognize the high-risk pattern.

Moreover, novel or existing agents could be tested, and their efficacy monitored with these methods. Here, preclinical disease models might come into play. Also, bone-active treatment could be tested within this framework.

When considering human studies, it is important to bear in mind that the natural history of a plaque spans, in most cases, over decades. With this information in mind, studies aimed at testing the efficacy of new treatment should be conceived so as to follow up the patient for an adequate stretch of time, before any conclusion can be drawn.

CONCLUSIONS

Radioisotope plaque imaging is a multi-faceted and promising field of research, which uses the newest available imaging methods to answer ancient questions, which regard the accurate risk estimation in the cardiovascular patient. Using these methods, inflammation and bone-forming activity can be identified and tracked within the atherosclerotic plaque, and a wide array of relevant information can be obtained.

In order to employ these techniques correctly, a standardization of the acquisition and analysis methods is urgently needed. Prospective randomized studied are also required to move this field from the purely academic area onto a patient-tailored diagnostic approach, having the potential to improve the quality of the cardiovascular diagnostic and to ameliorate the patients' survival and quality of life.

COMPLIANCE WITH ETHICAL REGULATIONS

All patients described in the present analyses signed an informed consent, which was approved by the Regional Review Board, before undergoing PET/CT imaging. This consent included the possibility of utilization of anonymized data in the framework of retrospective studies. Therefore, case-specific requirement for an approbation from the Ethics Committee was waived. Analysis was performed on an offline station, patients' names were pseudonomyzed. No study with animals was conducted.

ACKNOWLEDGMENTS

I would like to thank my family for the relentless support.

My heartfelt thanks go to the Prof. Sambuceti and to the Prof. Bagnasco for encouraging me to pursue this ambitious objective and to accept an important new challenge.

Special thanks to Dr. Piccardo and to Prof. Ciramiello for setting their own patient database at disposal and for contributing in reviewing my work.

REFERENCES

1 Laslett LJ, Alagona P, Jr., Clark BA, 3rd et al (2012) The worldwide environment of cardiovascular disease: prevalence, diagnosis, therapy, and policy issues: a report from the American College of Cardiology. J Am Coll Cardiol 60:S1-49

2 Collaborators GBDCoD (2017) Global, regional, and national age-sex specific mortality for 264 causes of death, 1980-2016: a systematic analysis for the Global Burden of Disease Study 2016. Lancet 390:1151-1210

3 Mortality GBD, Causes of Death C (2016) Global, regional, and national life expectancy, all-cause mortality, and cause-specific mortality for 249 causes of death, 1980-2015: a systematic analysis for the Global Burden of Disease Study 2015. Lancet 388:1459-1544

4 Foreman KJ, Marquez N, Dolgert A et al (2018) Forecasting life expectancy, years of life lost, and all-cause and cause-specific mortality for 250 causes of death: reference and alternative scenarios for 2016-40 for 195 countries and territories. Lancet 392:2052-2090

5 Chen S, Kuhn M, Prettner K, Bloom DE (2018) The macroeconomic burden of noncommunicable diseases in the United States: Estimates and projections. PLoS One 13:e0206702

6 Gheorghe A, Griffiths U, Murphy A, Legido-Quigley H, Lamptey P, Perel P (2018) The economic burden of cardiovascular disease and hypertension in low- and middle-income countries: a systematic review. BMC Public Health 18:975

7 Kannel WB, McGee D, Gordon T (1976) A general cardiovascular risk profile: the Framingham Study. Am J Cardiol 38:46-51

8 Silva DR, Werneck AO, Collings PJ et al (2017) Family history of cardiovascular disease and parental lifestyle behaviors are associated with offspring cardiovascular disease risk markers in childhood. Am J Hum Biol 29

9 D'Agostino RB, Sr., Vasan RS, Pencina MJ et al (2008) General cardiovascular risk profile for use in primary care: the Framingham Heart Study. Circulation 117:743-753

10 Nesto RW, Phillips RT (1986) Asymptomatic myocardial ischemia in diabetic patients. Am J Med 80:40-47

11 Kameyama M, Fushimi H, Udaka F (1994) Diabetes mellitus and cerebral vascular disease. Diabetes Res Clin Pract 24 Suppl:S205-208

12 Sakakura K, Nakano M, Otsuka F, Ladich E, Kolodgie FD, Virmani R (2013) Pathophysiology of atherosclerosis plaque progression. Heart Lung Circ 22:399-411

13 Otsuka F, Kramer MC, Woudstra P et al (2015) Natural progression of atherosclerosis from pathologic intimal thickening to late fibroatheroma in human coronary arteries: A pathology study. Atherosclerosis 241:772-782

14 Webber BJ, Seguin PG, Burnett DG, Clark LL, Otto JL (2012) Prevalence of and risk factors for autopsy-determined atherosclerosis among US service members, 2001-2011. JAMA 308:2577-2583

15 Hong YM (2010) Atherosclerotic cardiovascular disease beginning in childhood. Korean Circ J 40:1-9

16 Kligfield P, Lauer MS (2006) Exercise electrocardiogram testing: beyond the ST segment. Circulation 114:2070-2082

17 Gibbons RJ, Balady GJ, Bricker JT et al (2002) ACC/AHA 2002 guideline update for exercise testing: summary article. A report of the American College of Cardiology/American Heart Association Task Force on Practice Guidelines

(Committee to Update the 1997 Exercise Testing Guidelines). J Am Coll Cardiol 40:1531-1540
18 Maddahi J, Kiat H, Van Train KF et al (1990) Myocardial perfusion imaging with technetium-99m sestamibi SPECT in the evaluation of coronary artery disease. Am J Cardiol 66:55E-62E
19 Manda YR, Baradhi KM (2018) Cardiac Catheterization, Risks and ComplicationsStatPearls, Treasure Island (FL)
20 Jang IK, Bouma BE, Kang DH et al (2002) Visualization of coronary atherosclerotic plaques in patients using optical coherence tomography: comparison with intravascular ultrasound. J Am Coll Cardiol 39:604-609
21 Neves PO, Andrade J, Moncao H (2017) Coronary artery calcium score: current status. Radiol Bras 50:182-189
22 Greenland P, Bonow RO, Brundage BH et al (2007) ACCF/AHA 2007 clinical expert consensus document on coronary artery calcium scoring by computed tomography in global cardiovascular risk assessment and in evaluation of patients with chest pain: a report of the American College of Cardiology Foundation Clinical Expert Consensus Task Force (ACCF/AHA Writing Committee to Update the 2000 Expert Consensus Document on Electron Beam Computed Tomography) developed in collaboration with the Society of Atherosclerosis Imaging and Prevention and the Society of Cardiovascular Computed Tomography. J Am Coll Cardiol 49:378-402
23 Hou ZH, Lu B, Gao Y et al (2012) Prognostic value of coronary CT angiography and calcium score for major adverse cardiac events in outpatients. JACC Cardiovasc Imaging 5:990-999
24 Arbab-Zadeh A, Miller JM, Rochitte CE et al (2012) Diagnostic accuracy of computed tomography coronary angiography according to pre-test probability of coronary artery disease and severity of coronary arterial calcification. The CORE-64 (Coronary Artery Evaluation Using 64-Row Multidetector Computed Tomography Angiography) International Multicenter Study. J Am Coll Cardiol 59:379-387
25 Doherty TM, Fitzpatrick LA, Inoue D et al (2004) Molecular, endocrine, and genetic mechanisms of arterial calcification. Endocr Rev 25:629-672
26 Lloyd-Jones DM, Larson MG, Beiser A, Levy D (1999) Lifetime risk of developing coronary heart disease. Lancet 353:89-92
27 Libby P (2001) Current concepts of the pathogenesis of the acute coronary syndromes. Circulation 104:365-372
28 Qu W, Le TT, Azen SP et al (2003) Value of coronary artery calcium scanning by computed tomography for predicting coronary heart disease in diabetic subjects. Diabetes Care 26:905-910
29 Faxon DP, Fuster V, Libby P et al (2004) Atherosclerotic Vascular Disease Conference: Writing Group III: pathophysiology. Circulation 109:2617-2625
30 Libby P (2002) Inflammation in atherosclerosis. Nature 420:868-874
31 Rivard A, Andres V (2000) Vascular smooth muscle cell proliferation in the pathogenesis of atherosclerotic cardiovascular diseases. Histol Histopathol 15:557-571
32 Doherty TM, Asotra K, Fitzpatrick LA et al (2003) Calcification in atherosclerosis: bone biology and chronic inflammation at the arterial crossroads. Proc Natl Acad Sci U S A 100:11201-11206

33 Fiz F, Morbelli S, Piccardo A et al (2015) (1)(8)F-NaF Uptake by Atherosclerotic Plaque on PET/CT Imaging: Inverse Correlation Between Calcification Density and Mineral Metabolic Activity. J Nucl Med 56:1019-1023
34 Shah PK, Galis ZS (2001) Matrix metalloproteinase hypothesis of plaque rupture: players keep piling up but questions remain. Circulation 104:1878-1880
35 Silvera SS, Aidi HE, Rudd JH et al (2009) Multimodality imaging of atherosclerotic plaque activity and composition using FDG-PET/CT and MRI in carotid and femoral arteries. Atherosclerosis 207:139-143
36 Davies JR, Izquierdo-Garcia D, Rudd JH et al (2010) FDG-PET can distinguish inflamed from non-inflamed plaque in an animal model of atherosclerosis. Int J Cardiovasc Imaging 26:41-48
37 Tarkin JM, Joshi FR, Rudd JH (2014) PET imaging of inflammation in atherosclerosis. Nat Rev Cardiol 11:443-457
38 Tarkin JM, Joshi FR, Evans NR et al (2017) Detection of Atherosclerotic Inflammation by (68)Ga-DOTATATE PET Compared to [(18)F]FDG PET Imaging. J Am Coll Cardiol 69:1774-1791
39 Wan MYS, Endozo R, Michopoulou S et al (2017) PET/CT Imaging of Unstable Carotid Plaque with (68)Ga-Labeled Somatostatin Receptor Ligand. J Nucl Med 58:774-780
40 Derlin T, Wisotzki C, Richter U et al (2011) In vivo imaging of mineral deposition in carotid plaque using 18F-sodium fluoride PET/CT: correlation with atherogenic risk factors. J Nucl Med 52:362-368
41 Derlin T, Richter U, Bannas P et al (2010) Feasibility of 18F-sodium fluoride PET/CT for imaging of atherosclerotic plaque. J Nucl Med 51:862-865
42 Derlin T, Toth Z, Papp L et al (2011) Correlation of inflammation assessed by 18F-FDG PET, active mineral deposition assessed by 18F-fluoride PET, and vascular calcification in atherosclerotic plaque: a dual-tracer PET/CT study. J Nucl Med 52:1020-1027
43 George RT (2012) 18F-sodium fluoride positron emission tomography: an in vivo window into coronary atherosclerotic plaque biology. J Am Coll Cardiol 59:1549-1550
44 Fiz F, Morbelli S, Bauckneht M et al (2016) Correlation between thoracic aorta 18F-natrium fluoride uptake and cardiovascular risk. World J Radiol 8:82-89
45 Morbelli S, Fiz F, Piccardo A et al (2014) Divergent determinants of 18F-NaF uptake and visible calcium deposition in large arteries: relationship with Framingham risk score. Int J Cardiovasc Imaging 30:439-447
46 Joshi NV, Vesey AT, Williams MC et al (2014) 18F-fluoride positron emission tomography for identification of ruptured and high-risk coronary atherosclerotic plaques: a prospective clinical trial. Lancet 383:705-713
47 Sambuceti G, Brignone M, Marini C et al (2012) Estimating the whole bone-marrow asset in humans by a computational approach to integrated PET/CT imaging. Eur J Nucl Med Mol Imaging 39:1326-1338
48 Pencina MJ, D'Agostino RB, Sr., Larson MG, Massaro JM, Vasan RS (2009) Predicting the 30-year risk of cardiovascular disease: the framingham heart study. Circulation 119:3078-3084
49 Ackerhalt RE, Blau M, Bakshi S, Sondel JA (1974) A comparative study of three 99mTc-labeled phosphorus compounds and 18F-fluoride for skeletal imaging. J Nucl Med 15:1153-1157
50 Thrall JH (1976) Technetium-99m labeled agents for skeletal imaging. CRC Crit Rev Clin Radiol Nucl Med 8:1-31

51 Minamimoto R, Loening A, Jamali M et al (2015) Prospective Comparison of 99mTc-MDP Scintigraphy, Combined 18F-NaF and 18F-FDG PET/CT, and Whole-Body MRI in Patients with Breast and Prostate Cancer. J Nucl Med 56:1862-1868
52 Dweck MR, Chow MW, Joshi NV et al (2012) Coronary arterial 18F-sodium fluoride uptake: a novel marker of plaque biology. J Am Coll Cardiol 59:1539-1548
53 Lee JM, Bang JI, Koo BK et al (2017) Clinical Relevance of (18)F-Sodium Fluoride Positron-Emission Tomography in Noninvasive Identification of High-Risk Plaque in Patients With Coronary Artery Disease. Circ Cardiovasc Imaging 10
54 Dweck MR, Jenkins WS, Vesey AT et al (2014) 18F-sodium fluoride uptake is a marker of active calcification and disease progression in patients with aortic stenosis. Circ Cardiovasc Imaging 7:371-378
55 Li X, Heber D, Cal-Gonzalez J et al (2017) Association Between Osteogenesis and Inflammation During the Progression of Calcified Plaque Evaluated by (18)F-Fluoride and (18)F-FDG. J Nucl Med 58:968-974
56 Ishiwata Y, Kaneta T, Nawata S, Hino-Shishikura A, Yoshida K, Inoue T (2017) Quantification of temporal changes in calcium score in active atherosclerotic plaque in major vessels by (18)F-sodium fluoride PET/CT. Eur J Nucl Med Mol Imaging 44:1529-1537
57 Bagger YZ, Tanko LB, Alexandersen P, Qin G, Christiansen C, Prospective Epidemiological Risk Factors Study G (2006) Radiographic measure of aorta calcification is a site-specific predictor of bone loss and fracture risk at the hip. J Intern Med 259:598-605
58 Farhat GN, Newman AB, Sutton-Tyrrell K et al (2007) The association of bone mineral density measures with incident cardiovascular disease in older adults. Osteoporos Int 18:999-1008
59 Samelson EJ, Miller PD, Christiansen C et al (2014) RANKL inhibition with denosumab does not influence 3-year progression of aortic calcification or incidence of adverse cardiovascular events in postmenopausal women with osteoporosis and high cardiovascular risk. J Bone Miner Res 29:450-457
60 Fiz F, Marini C, Campi C et al (2015) Allogeneic cell transplant expands bone marrow distribution by colonizing previously abandoned areas: an FDG PET/CT analysis. Blood 125:4095-4102
61 Fiz F, Marini C, Piva R et al (2014) Adult advanced chronic lymphocytic leukemia: computational analysis of whole-body CT documents a bone structure alteration. Radiology 271:805-813
62 Fiz F, Sahbai S, Campi C et al (2017) Tumor Burden and Intraosseous Metabolic Activity as Predictors of Bone Marrow Failure during Radioisotope Therapy in Metastasized Prostate Cancer Patients. Biomed Res Int 2017:3905216
63 Pasha AK, Moghbel M, Saboury B et al (2015) Effects of age and cardiovascular risk factors on (18)F-FDG PET/CT quantification of atherosclerosis in the aorta and peripheral arteries. Hell J Nucl Med 18:5-10